TR No. 124

THE UNIVERSITY OF MICHIGAN

DEPARTMENT OF ELECTRICAL ENGINEERING

COOLEY ELECTRONICS LABORATORY

Technical Report No. 124

Remotely-Controlled Tactical Direction-Finding System

By: E. M. AUPPERLE
T. W. BUTLER, JR.
D. L. MILLS

Approved by: B. F. BARTON

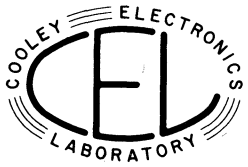

Under Contract With:

CONTRACT NO. DA-36-039 sc-78283 DEPARTMENT OF ARMY
PROJECT NO. 3A99-06-001-01 PLACED BY: U. S. ARMY
SIGNAL RESEARCH AND DEVELOPMENT LABORATORY,
FORT MONMOUTH, N. J.

Administered through:

July 1961

OFFICE OF RESEARCH ADMINISTRATION • ANN ARBOR

THE UNIVERSITY OF MICHIGAN
OFFICE OF RESEARCH ADMINISTRATION
ANN ARBOR

REMOTELY-CONTROLLED TACTICAL DIRECTION-FINDING SYSTEM

Technical Report No. 124
2899-58-T

Cooley Electronics Laboratory
Department of Electrical Engineering

By: E. M. Aupperle
T. W. Butler, Jr.
D. L. Mills

Approved by: B. F. Barton

Project 2899

TASK ORDER NO. EDG-4
CONTRACT NO. DA-36-039 sc-78283
SIGNAL CORPS, DEPARTMENT OF THE ARMY
DEPARTMENT OF THE ARMY PROJECT NO. 3A99-06-001-01

July 1961

ABSTRACT

This report summarizes the work leading to the conception, design, and development of a receiver system employing solid-state tuning for use in a remotely-controlled direction-finding application. The cardinal features of the system are:

1) The elimination of the man at remote stations.
2) Accurate station identification.
3) Short acquisition times.
4) Good system-wide frequency stability.

Included is a detailed description of the basic receiver and supporting telemetry and antenna subsystems.

TABLE OF CONTENTS

LIST OF ILLUSTRATIONS

LIST OF ILLUSTRATIONS (Cont.)

ACKNOWLEDGEMENTS

In the work reported here, the authors have been influenced greatly by their association with the other members of the Cooley Electronics Laboratory. In particular, Mr. G. A. Roberts contributed much to the proposals of the various systems considered in Section 2. The authors are indebted to Mr. H. Burr and Mr. C. Rockafellow for their assistance in system development. Credit is also due Mr. W. Nelson for his work in building the experimental equipment.

REMOTELY-CONTROLLED TACTICAL DIRECTION-FINDING SYSTEM

1. INTRODUCTION

In the tactical environment of the battlefield there is a need for a compact direction-finding system with the capability of complete control by the master station. The advantages of such a system as compared to existing DF nets may include the following: (1) the elimination of the man at remote stations, (2) shorter acquistion times, (3) good system-wide frequency stability, and (4) accurate station identification. As a consequence of the above-mentioned need coupled with the recent developments in voltage-controlled, solid-state tuning elements, it was decided to evaluate the feasibility of a Remotely-Controlled Tactical Direction-Finding System as an application of solid-state devices.

The heart of any direction finding system is the basic receiver. This report briefly summarizes the five alternative receiver concepts which were initially proposed. Following this summary a detailed description of the design, performance, and evaluation of one of these concepts is presented. This report also contains information on the design and evaluation of the supporting telemetry and antenna subsystems which were built to demonstrate the total DF system.

As an outgrowth of the work on the DF receiver a number of side benefits quickly resulted. These included the conceptual design and prototype development of a Generalized Frequency Synthesizer discussed in Technical Report No. 120 (Ref. 1) and the realization that the basic DF receiver had several unique and useful characteristics which provide it with a more general utility. To elaborate on this

last point it will be observed from this report that the DF receiver has the following properties:

(a) High set-on accuracy.

(b) No moving parts.

(c) Fast frequency selection.

(d) Low data-rate control channels for remote operation.

(e) Light weight and compact design.

(f) Only one crystal for complete frequency control.

Applications of this type of receiver include ground, airborne, missile, and satellite communication systems in which rapid but precise frequency selection is necessary. These include, for example:

(a) The simultaneous operation of several slave receivers at remote locations as required in remotely-controlled direction-finding nets.

(b) Use in frequency-hopping pseudo-random communication systems in which the receiver is operating in conjunction with a synchronized transmitter.

(c) As a two-station, time-sharing receiver for compatible monophonic or stereo reception.

(d) In airborne navigation systems requiring fast selection of predetermined channels (e.g., the omni-range system).

(e) To reduce the effect of deep fades in long-range communication systems by selective frequency hopping.

2. AN OUTLINE OF FIVE POSSIBLE TACTICAL DF RECEIVERS USING SOLID-STATE TUNING

The tactical situation for which the following receiver con-

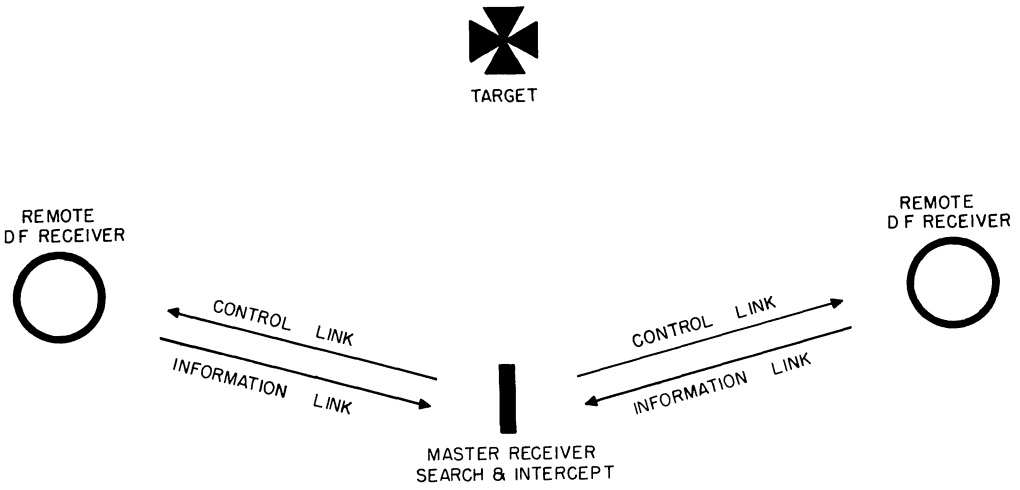

Fig. 1. Tactical situation.

cepts are proposed is depicted in Fig. 1. In each case the complete system consists of a manually-controlled master station with two (or more) remote DF sites. The **control** link is used to transmit control functions from the master to the remote stations, while the information link returns the video and antenna bearing information to the master station for data processing. It is intended that the control and information linkages be made compatible to either radio or wire transmission.

All of the receivers presented in the block diagrams which follow **employ** solid-state tuning elements (i.e., ferroelectric capacitors), back-biased diode capacitors, or controllable inductors in the tunable stages at both the master and remote stations).

2.1 System A (Refer to block diagram, Fig. 2).

System A employs simple, open-loop receivers. Each remote and master receiver must be tuned manually from the control site. It is necessary to monitor each receiver frequently to assure proper tuning.

Functions Transmitted on Control Link:

1) RF and mixer tuning voltages.

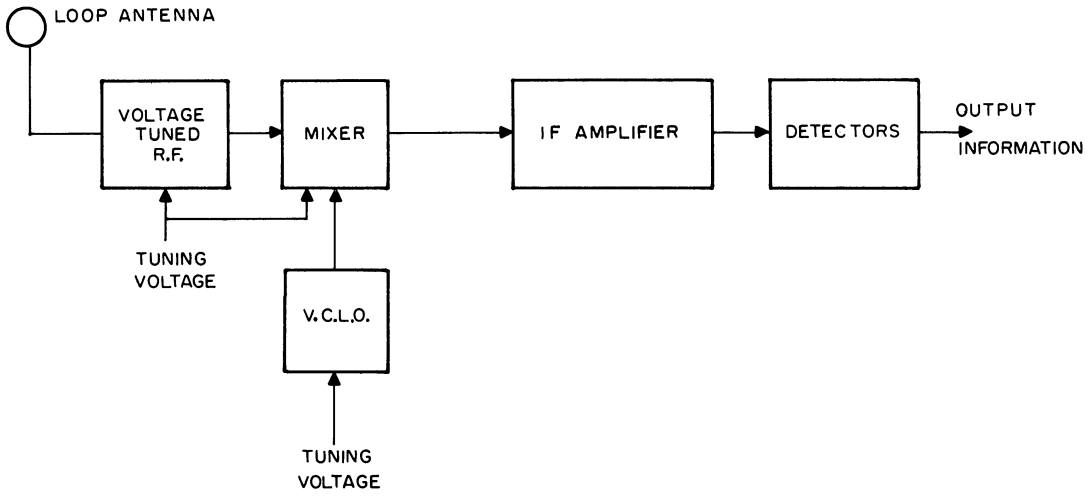

Fig. 2. Remote-tuned DF receiver (system A).

2) Voltage-controlled local oscillator (VCLO) tuning voltage.

3) On-off.

4) Gain control.

5) Antenna control.

Functions Received on Information Link:

1) Video.

2) Antenna position.

Advantages:

1) Simplicity of total system.

2) Low power consumption.

3) Narrow bandwidth control channels.

Disadvantages:

1) Heavy burden on master station controller for tuning.

2) Item 1 implies a long acquisition time.

3) Short time drift.

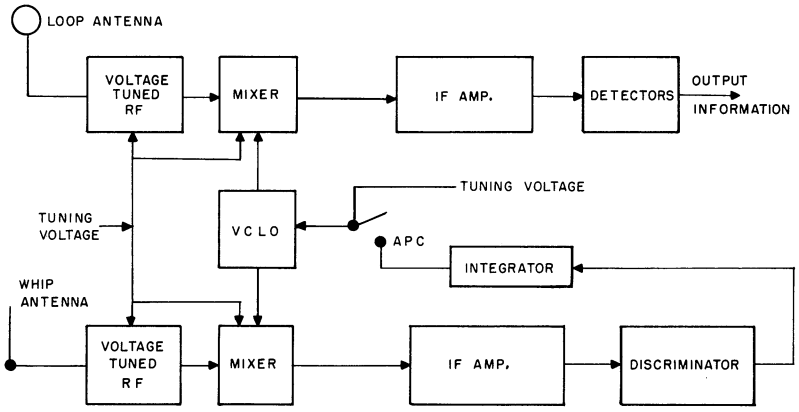

Fig. 3. Remote-tuned DF receiver (System B).

2.2 System B (Refer to block diagram, Fig. 3.)

In System B each receiver contains a "search-and-hold" unit in addition to the direction-finding unit. In operation, both units in each receiver are tuned simultaneously by the operator in the same manual fashion as in System A. When a particular signal is obtained, the receiver can be switched to a holding mode employing the automatic phase control (APC) feature.

Functions Transmitted on Control Link:

1) All functions listed for System A.

2) Tune - Automatic Phase Control Switch

Advantages:

1) Alleviates short time drift compared to System A.

2) Since the remote receiver is locked to the signal being monitored the burden on the master station controller is not as heavy.

Disadvantages:

1) The acquisition time is as long as in System A.

2) If the signal being monitored drops below some low level,

adjacent strong signals may capture the receiver. However, the operator has the option of defeating the APC and returning to manual tune as described in System A.

3) Once a transmitter is turned off it is generally necessary to relock the various receivers in the net on the next transmission. Hence, for short burst signals this system has no advantage over System A.

4) This system has approximately twice the complexity of System A.

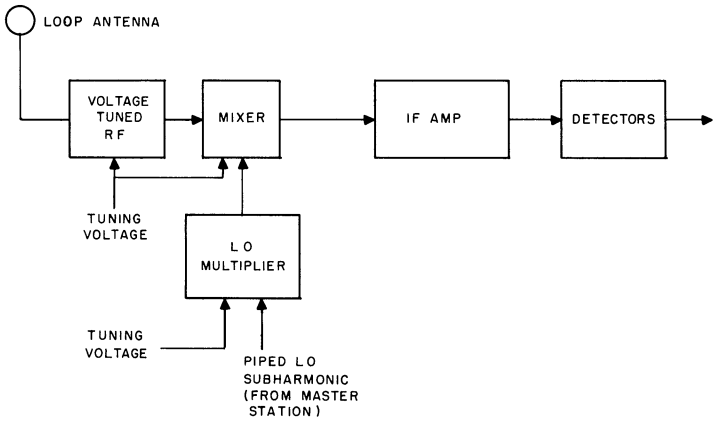

Fig. 4. Remote-tuned DF receiver (System C).

2.3 System C (Refer to block diagram, Fig. 4.)

The scheme in System C employs a crystal-controlled local oscillator (LO) in the master receiver. Each remote receiver is then supplied with a subharmonic of the master LO and a tuning voltage to adjust the LO frequency multiplier. This technique assures precise station identification.

Functions Transmitted on Control Link:

1) RF and mixer tuning voltages.

2) A subharmonic of the master local oscillator, one which is

below 10 Mc so that excessive transmission line loss would not be encountered.

3) Local oscillator multiplier tuning voltages.

4) Gain control.

5) On-off.

6) Antenna control.

Functions Received on Information Link:

1) Same as above systems.

Advantages:

1) Since the local oscillator is "piped" from the master receiver to each remote location, precise station identification is possible.

2) Short acquisition times are possible, restricted only by the time constants of the multiplier circuitry.

3) Excellent system-wide frequency stability.

Disadvantages:

1) Greater tendency for spurious responses due to the number of harmonic amplifiers used in the LO circuit.

2) Moderate complexity.

3) Transmission of control information by cable would be difficult due to bandwidth required for the LO subharmonic.

4) High-power control link needed for transmission of LO subharmonic to obtain a clean signal.

2.4 System D (Refer to block diagram, Fig. 5.)

This receiver design is somewhat more complex than the previous three and as a result might not be easily grasped from simply an inspection of the block diagram and a brief statement. A detailed description of its operation is given

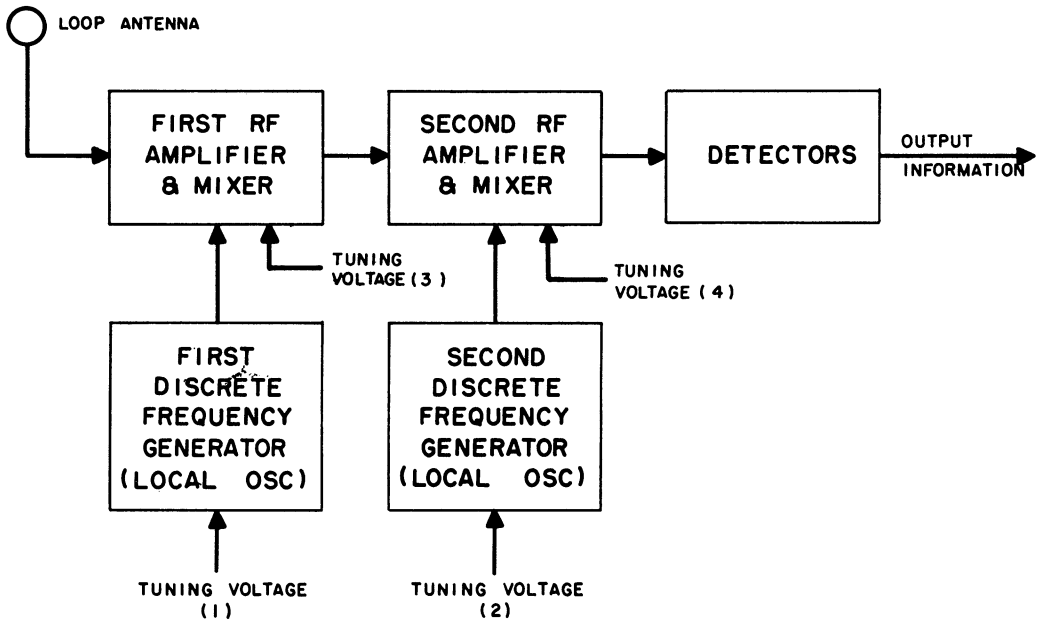

Fig. 5. Remote-tuned DF receiver (System D).

in Section 3.

Functions Transmitted on Control Link:

1) Two RF and mixer tuning voltages.

2) Two LO tuning voltages.

3) Gain control.

4) On-off.

5) Antenna control.

Functions Received on Information Link:

1) Same as other systems.

Advantages:

1) Accurate station identification is possible.

2) Good system-wide frequency stability.

3) Fast acquisition time.

4) Narrow bandwidth control links.

Disadvantages:

1) Tendency toward spurious responses due to harmonic genera-

tion.

2) Greater system complexity.

3) More control channels required than other systems.

4) Greater power consumption.

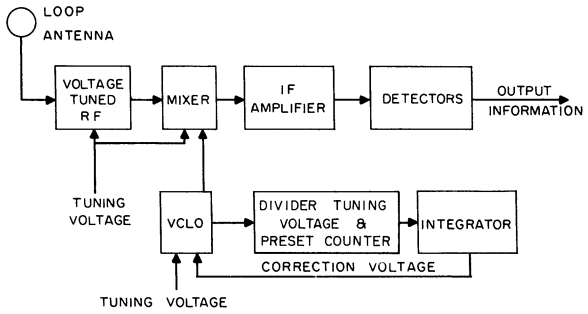

Fig. 6. Remote-tuned DF receiver (System E).

2.5 System E (Refer to block diagram, Fig. 6.)

In each receiver of System E the VCLO frequency is sampled by a counter and compared with a remotely supplied preset value. The error signal that is sensed is used to supply a local correction voltage.

Functions Transmitted on Control Link:

1) RF and mixer tuning voltages.

2) LO tuning voltages.

3) Preset counter voltages.

4) Gain control.

5) On-off.

6) Antenna control.

Functions Received on Information Link:

1) Same as above systems.

Advantages:

1) Accurate station identification is possible.

2) Good system-wide frequency stability.

3) Reasonable acquisition time.

4) Narrow bandwidth control link.

Disadvantages:

1) System complexity.

2) Considerable power consumption.

3) Physically large system.

2.6 Selection of System For Experimental Verification:

Since it was impossible to experimentally evaluate all of these systems some decision as to a reasonable experimental program had to be made. Receiver System A is by far the simplest, but the most demanding on the master station. It was felt that a more sophisticated system should be initially investigated. It is to be noted that both Systems B and D contain A as a subsystem.

System C was rejected due to the requirement of a high-power, wideband control link. The final system, E, was considered impractical at the time because of the complexity of high-speed, physically small counters.

The choice between Systems B and D was not so simple. The two schemes are completely different in concept and both have distinct advantages. The decision was made in favor of System D primarily because it is a less commonly encountered receiver concept, and it has several unique and useful characteristics.

3. RECEIVER SUBSYSTEM

3.1 Background Notes

The inclusion of solid-state tuning elements[1] in resonant circuits permits the construction of physically small, light weight, inexpensive, and electrically simple voltage controlled oscillators (VCO's) and RF amplifiers. A major fault of these tuning elements is their lack of precision (i.e., dependence on temperature and voltage). For this basic reason a VCO is rarely found as the local oscillator in a conventional receiver. Nevertheless, the combination of mechanical and solid-state tuning is currently employed in many commercial FM tuners to provide the gross frequency adjust (mechanical) and frequency drift control via a simple AFC circuit (solid-state).

The many desirable properties of solid-state tuning induce the circuit designer to search for techniques which will either actively control or at least compensate for the basic lack of precision. This report will present a scheme in which a VCO is utilized in conjunction with a master frequency standard (e.g., a crystal) of arbitrary accuracy to provide a tunable oscillator for a receiver with the same accuracy. This is accomplished by literally locking the VCO to the various harmonics of the frequency standard. The resultant local oscillator is therefore discretely tunable over its operational range.

3.2 Conceptual Design

The first aspect of the receiver subsystem introduced in this section is the basic converter module, including a qualitative description

---

[1] Ferroelectric capacitors, back-biased diode capacitors, and controllable inductors.

of the discrete frequency generator. Following this is a discussion on the implementation of two converter modules in a complete receiver subsystem. This section concludes with a flow chart to facilitate the understanding of how signals are processed by the receiver.

A block diagram for the basic receiver converter module is depicted in Fig. 7. The incoming signal is processed by an RF amplifier

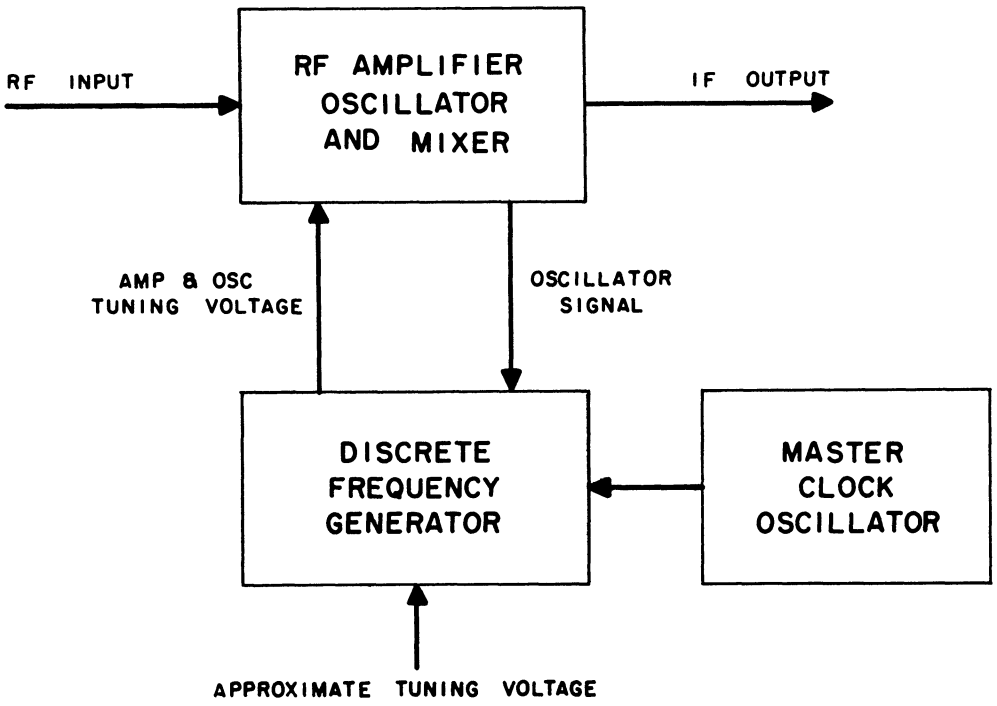

Fig. 7. Basic converter module.

and mixer in a conventional superheterodyne configuration. The local oscillator voltage is simultaneously applied to the mixer and to a discrete-frequency generator (DFG). In the DFG, the unique feature of this design, the local oscillator frequency is compared with a harmonic of a master clock oscillator. Unless there is zero frequency difference between the local oscillator and the harmonic, a time-varying voltage is

generated by a comparator circuit. The resulting error voltage is added to the approximate tuning voltage (used to coarsely tune the oscillator to the desired harmonic) and causes the local oscillator to be frequency modulated. If the approximate tuning voltage was initially able to tune the local oscillator sufficiently close (in frequency) to the desired harmonic, then the error signal is able to "lock" the oscillator to the harmonic.

To obtain a more detailed understanding of the DFG refer to Fig. 8. Observe that the output of the master clock oscillator (with a

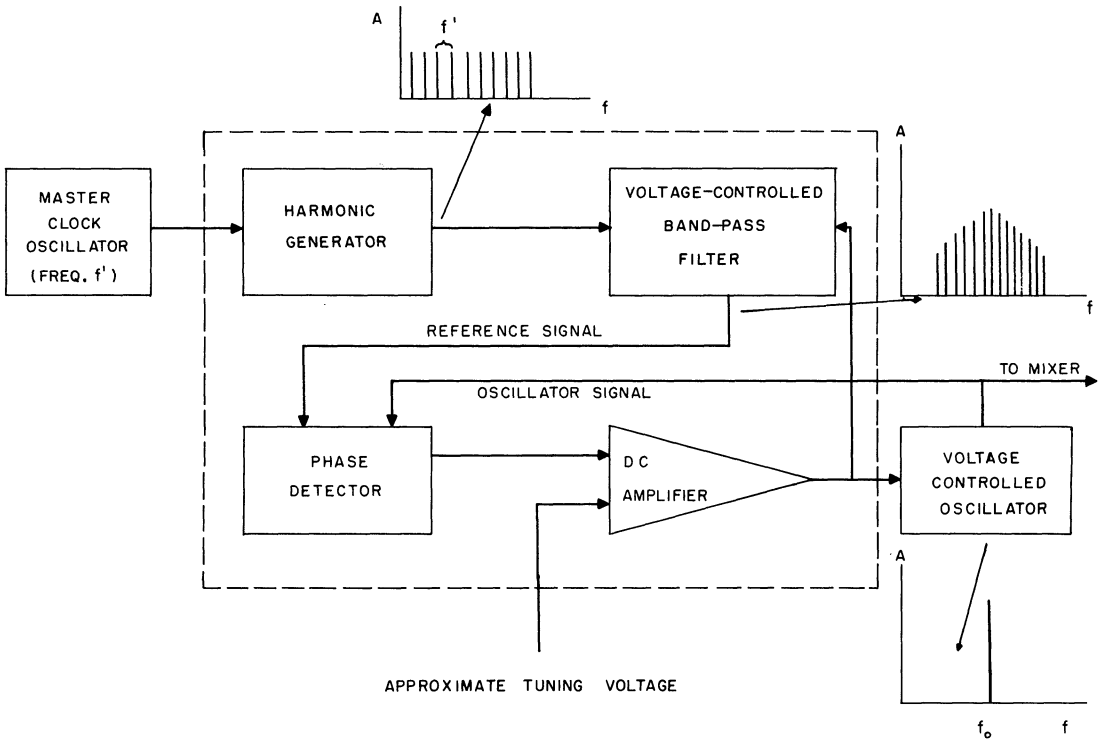

Fig. 8. Discrete-frequency generator (DFG).

frequency f') is applied to a harmonic generator. This harmonic generator in turn produces a periodic voltage with a Fourier frequency spectrum as shown in Fig. 8. Typically, only a few of the resulting harmonics are

required, and these are selectively obtained by filtering. Thus, at this point there exists a set of harmonics spaced every f' cycles between some upper and lower limit determined by the filter. This is called the reference signal.

Along with the reference signal, the local oscillator is also applied to the phase detector. Fig. 8 shows the way in which the local oscillator is grossly tuned by the application of an approximate tuning voltage. The tolerance of this approximate tuning voltage is specified by the necessity for unambiguous selection of adjacent harmonics. Once the oscillator is tuned sufficiently close to a given harmonic, an error signal is obtained from the phase detector. This error voltage serves to alter the frequency of the local oscillator continuously until zero difference frequency is achieved; at which time a constant error voltage is maintained to keep the local oscillator in lock. A mathematical description of the above operation is given in Appendix A.

To summarize the discussion of the converter module, Fig. 9 was prepared. It shows in detail the functions presented in Fig. 7. The same control voltage supplied to the oscillator is used to tune the RF amplifier as well as the band-pass filter in the DFG. This is by no means necessary, but the single tuning voltage is desirable from a practical standpoint.

To facilitate the following discussion certain parameters of the experimental receiver subsystem will be introduced:[1]

---

[1] A complete list of the DF receiver specifications is given on page 19.

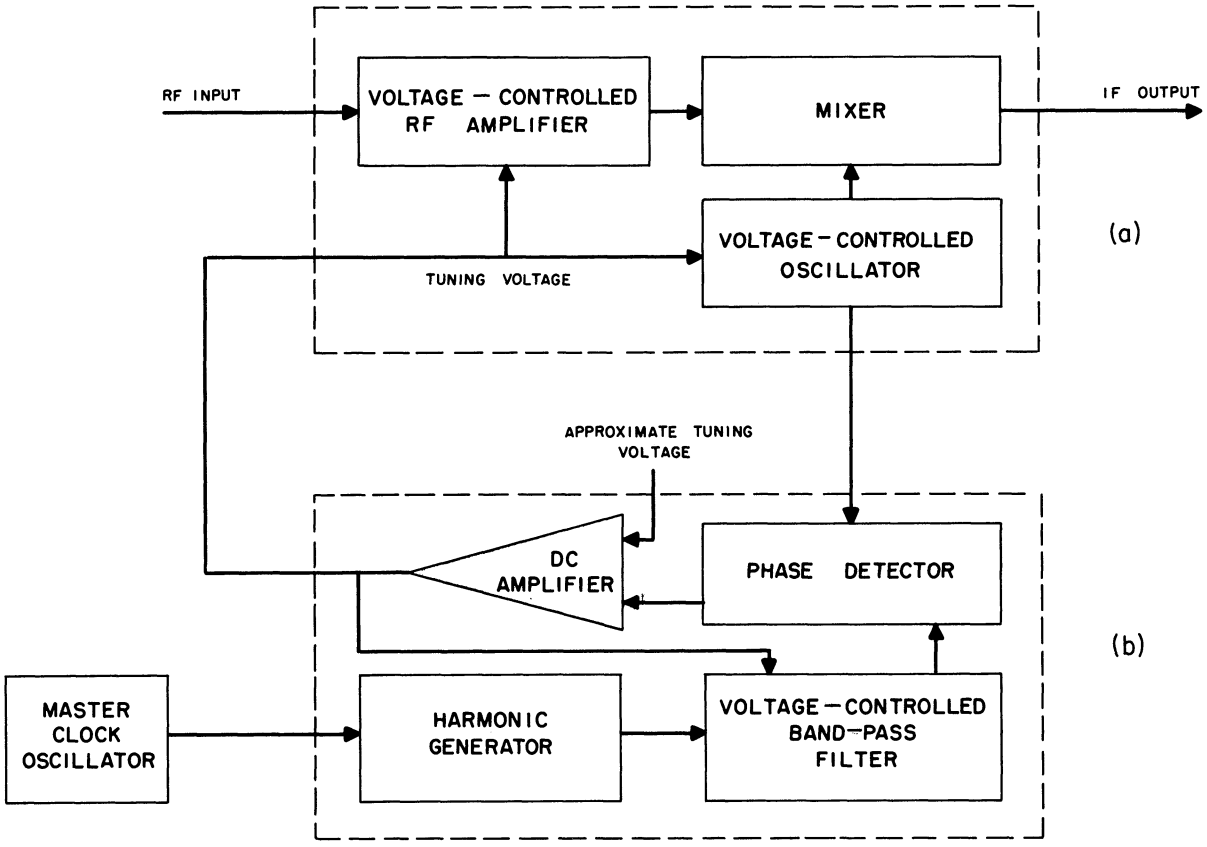

Fig. 9. Detailed converter module diagram.

Frequency Range	Input	80-102 Mc	(tuned in 11 2-Mc steps)
	1st IF	18-20 Mc	(tuned in 20 100-kc steps)
	2nd IF	4.5 Mc	
Bandwidth	Input	2 Mc	
	1st IF	100 kc	
	2nd IF	100 kc	

These figures represent a reasonable compromise between state-of-the-art capability and practical DF receiver requirements. In particular, the relatively narrow frequency range (80-102 Mc) was selected to simplify the tuning problem. It is to be noted that the present upper limit on tuning range for diode and ferroelectric capacitors is approxi-

mately 2-1/2 to 1 in frequency.

Based on the above parameters and the previously described converter module, the experimental receiver block diagram is presented in Fig. 10. This receiver employs two converter modules to obtain 220 discrete local oscillator settings spaced at 100-kc intervals. Note that the same master oscillator is used to provide the basic frequency reference for both DFG's. Conventional AM and FM detection circuits and a control panel complete the receiver. It is to be noted that this receiver design will function equally well with other forms of modulation (e.g., SSB, DSBSC, etc.) if an appropriate detector is provided.

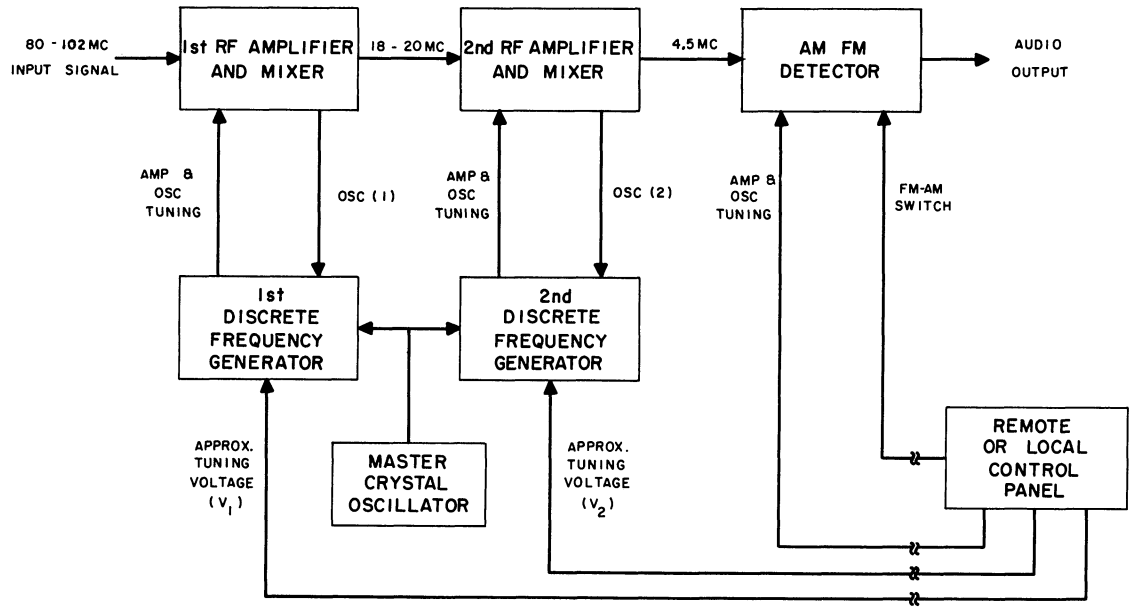

Fig. 10. Block diagram of experimental receiver.

The operation of this receiver is as follows: The intercepted signal is applied to a 2-Mc-wide amplifier to provide both RF sensitivity

and image rejection. The signal is then mixed with a discretely-tuned local oscillator with a frequency of 2M Mc (here M is an integer in the range $50 \leq M \leq 60$) to produce a difference frequency from 18 to 20 Mc. The selection of a particular value of M is determined by the dc voltage, V_1.

At this point in the receiver all the signals in a specified 2-Mc region of the 80-102 Mc band are available for further processing. The second converter selects a 100-kc segment of the 18-20 Mc band. This is done by amplifying the desired signal to obtain sufficient image rejection and then mixing with a discretely chosen frequency given by N/10 Mc (here N is an integer in the range $225 \leq N \leq 245$). The output frequency of this second converter is 4.5 Mc with a 100-kc bandwidth, and the local oscillator frequency is determined by the tuning voltage, V_2. Thus at this point the receiver has a 100-kc selectivity and is capable of tuning any signal from 80 to 102 Mc whose carrier is a harmonic of 100 kc, i.e., 80.0, 80.1, 80.2, ..., 101.9, 102.0 Mc. The frequency stability is completely determined by the master clock oscillator.

Since all commercial FM stations have their carriers spaced in 200-kc intervals between 88.1 and 107.9 Mc, it was convenient simply to process the 4.5 Mc output by a conventional FM IF and detector circuit. For AM signals, the remainder of the receiver is essentially a standard broadcast-band tuner with a continuously-variable, voltage-tunable oscillator covering the range 4.955 to 5.055 Mc. This produces a 455-kc IF frequency which is amplified and then detected.

To give the reader a clearer understanding of how signals are processed by this multi-conversion receiver, Fig. 11 was prepared. To demonstrate the use of this chart, consider the following example.

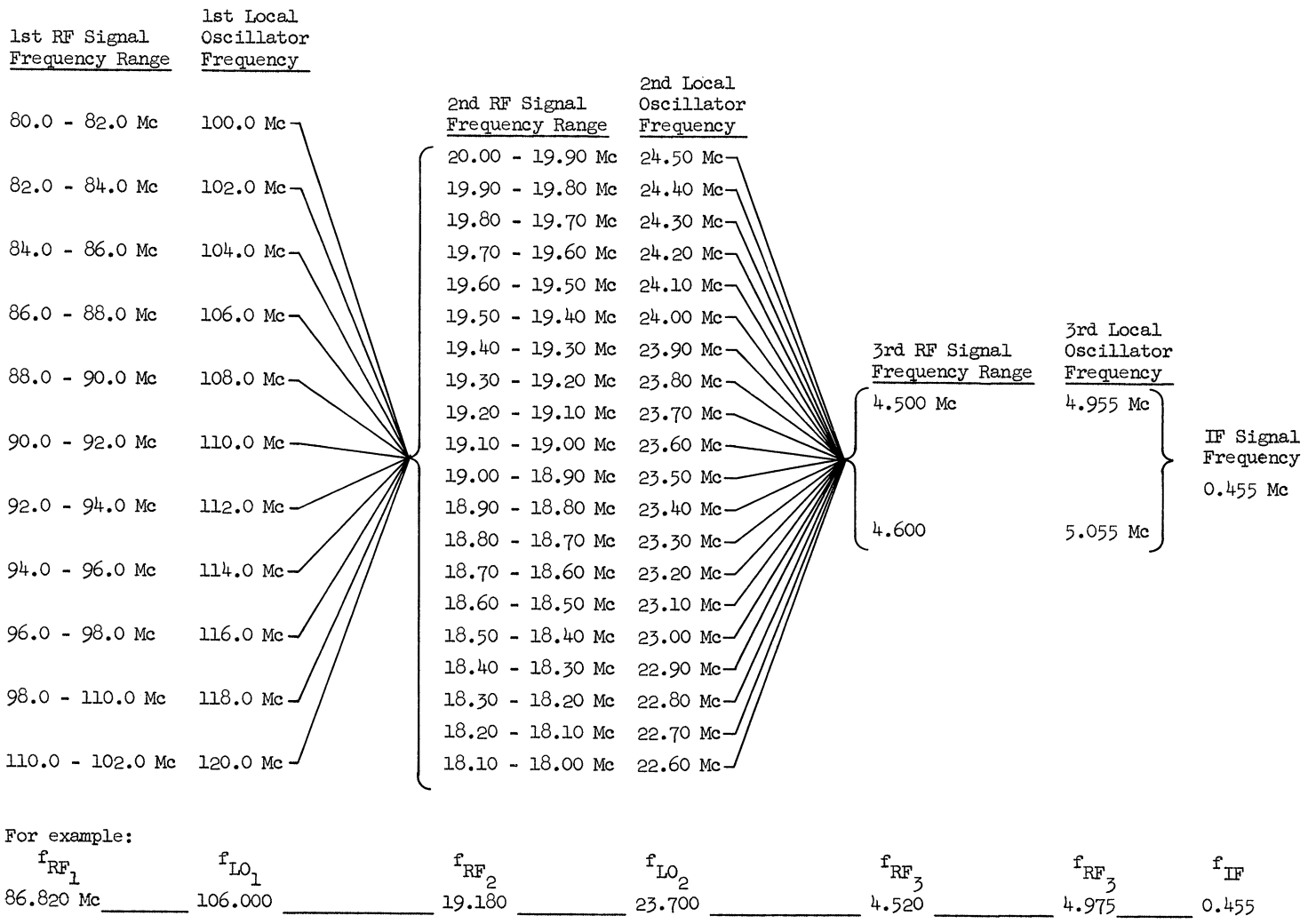

Fig. 11. Frequency conversion flow diagram of DF receiver.

Example Given an AM carrier at 86.820 Mc, how is the signal processed? Referring to Fig. 11, it can be seen that the signal falls between 86.0 and 88.0 Mc and hence will be mixed with a local oscillator signal of 106.000 Mc to produce a converted frequency within the 18.0 to 20-Mc band. The 19.180-Mc frequency falls between 19.10 and 19.20 Mc and hence will beat with a 23.700-Mc local oscillator to yield 4.520 Mc. This is mixed with 4.975 Mc to give an IF frequency of 0.455 Mc.

3.3 A Discussion of the Experimental Receiver Circuit

To demonstrate the feasibility of the receiver scheme described in the previous section an experimental unit was constructed. The complete list of design parameters is as follows:

Frequency Range	Input	80-102 Mc	
	1st IF	18-20 Mc	
	2nd IF	4.5-4.6 Mc	
	3rd IF	0.455 Mc	(AM only)
Bandwidth	Input	2 Mc	
	1st IF	100 kc	
	2nd IF	100 kc	
	3rd IF	25 kc	(AM only)
Image Rejection	80 db		
Sensitivity	0.5 Microvolts		

It is convenient to examine and discuss the experimental receiver based on the block diagram shown previously in Fig. 10. There is a one-to-one correspondence of the blocks in this figure to the physical layout of the receiver. The following paragraphs will briefly describe the implementation of these various blocks with the emphasis given to

the significant and unique aspects of the design.[1]

Consider first the AM and FM detector block. This unit employs conventional circuitry in all respects except for the AM local oscillator. Here the mechanically-variable capacitor was replaced by an electrically-controlled diode capacitor. The tuning characteristic of this local oscillator is given in Fig. 12 with frequency plotted vs. tuning bias. A manual switch is currently employed to select the detection mode. The IF strips as required are 100 kc and 25 kc wide, respectively, for the FM and AM channels.

Next in line are the two RF amplifier and mixer blocks. With the exception of frequency coverage and minor circuit variations these units are similar. Each contains a three-stage, voltage-tuned RF amplifier section to provide the required 80-db image rejection. These amplifiers employ 6AK5 tubes in a grounded cathode circuit with diode capacitors in the interstage networks. No attempt was made to obtain a low noise figure configuration on the front end of either unit. It was necessary to employ high-Q diodes ($Q < 50$ at 50 Mc) to obtain the desired 2-Mc over-all bandwidth of the high-frequency RF amplifier. The input, as well as output, impedance for both of these converter blocks was designed to be 50 ohms.

Besides the amplifier section, both units employ 6BE6 pentagrid converters operating with separate excitation. The local oscillator signal is supplied by a voltage-tuned oscillator contained in the same chassis for maximum coupling efficiency. Since it is necessary to bring both the oscillator voltage and the converted signal out of these blocks, a final

---

[1] A complete set of circuit prints of the receiver is given in Appendix B.

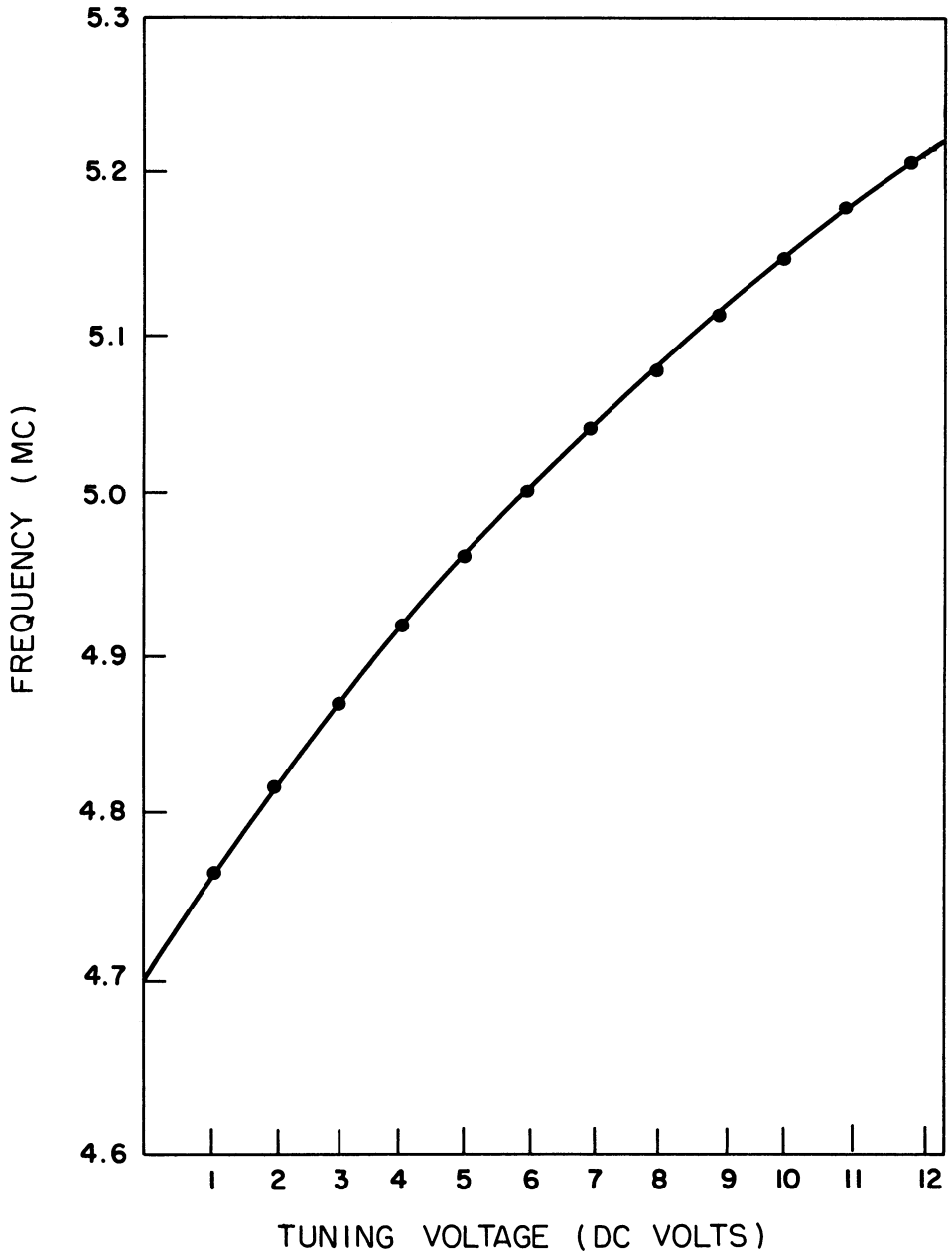

Fig. 12. Low frequency oscillator curve.

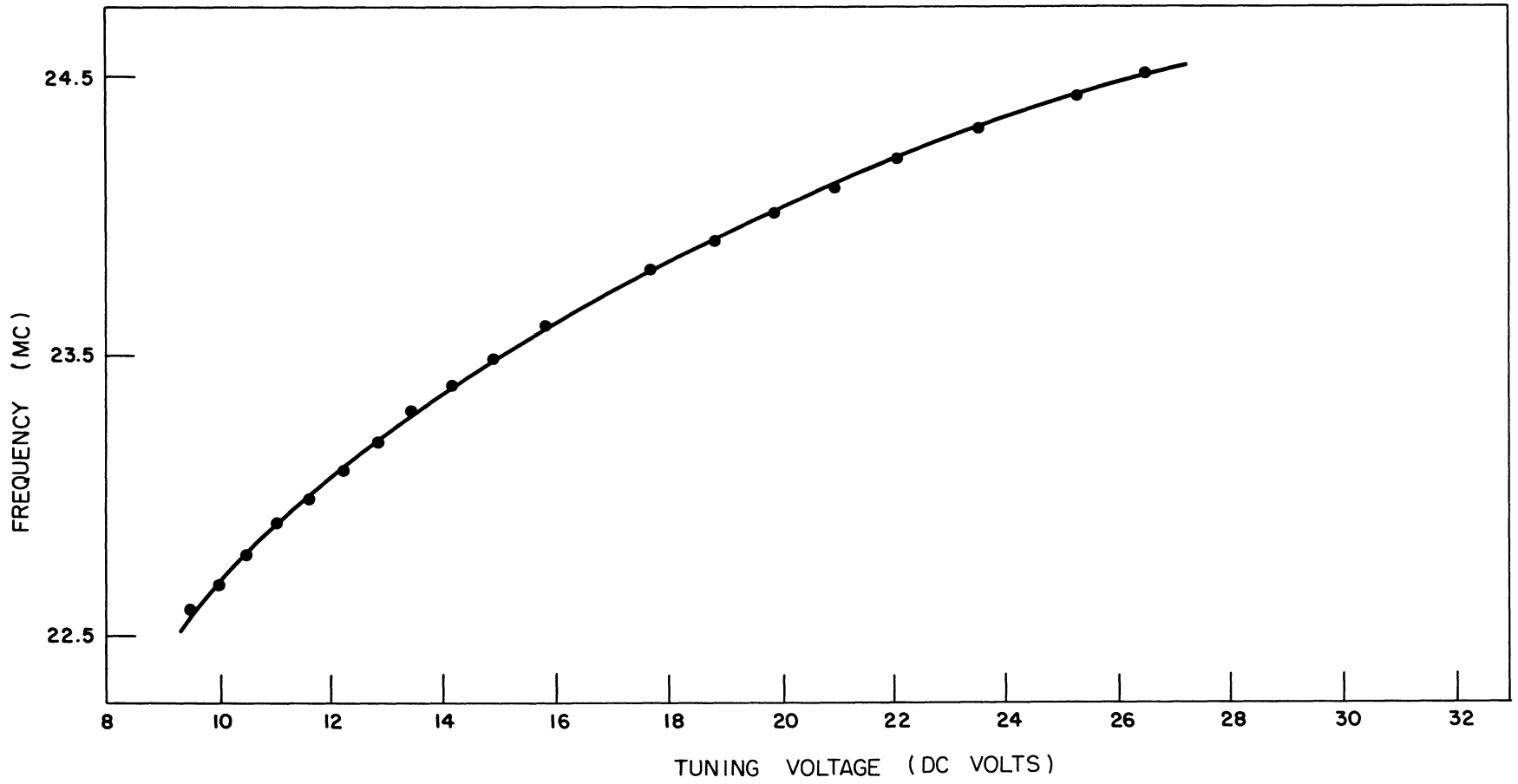

Fig. 13. Intermediate - frequency oscillator tuning curve.

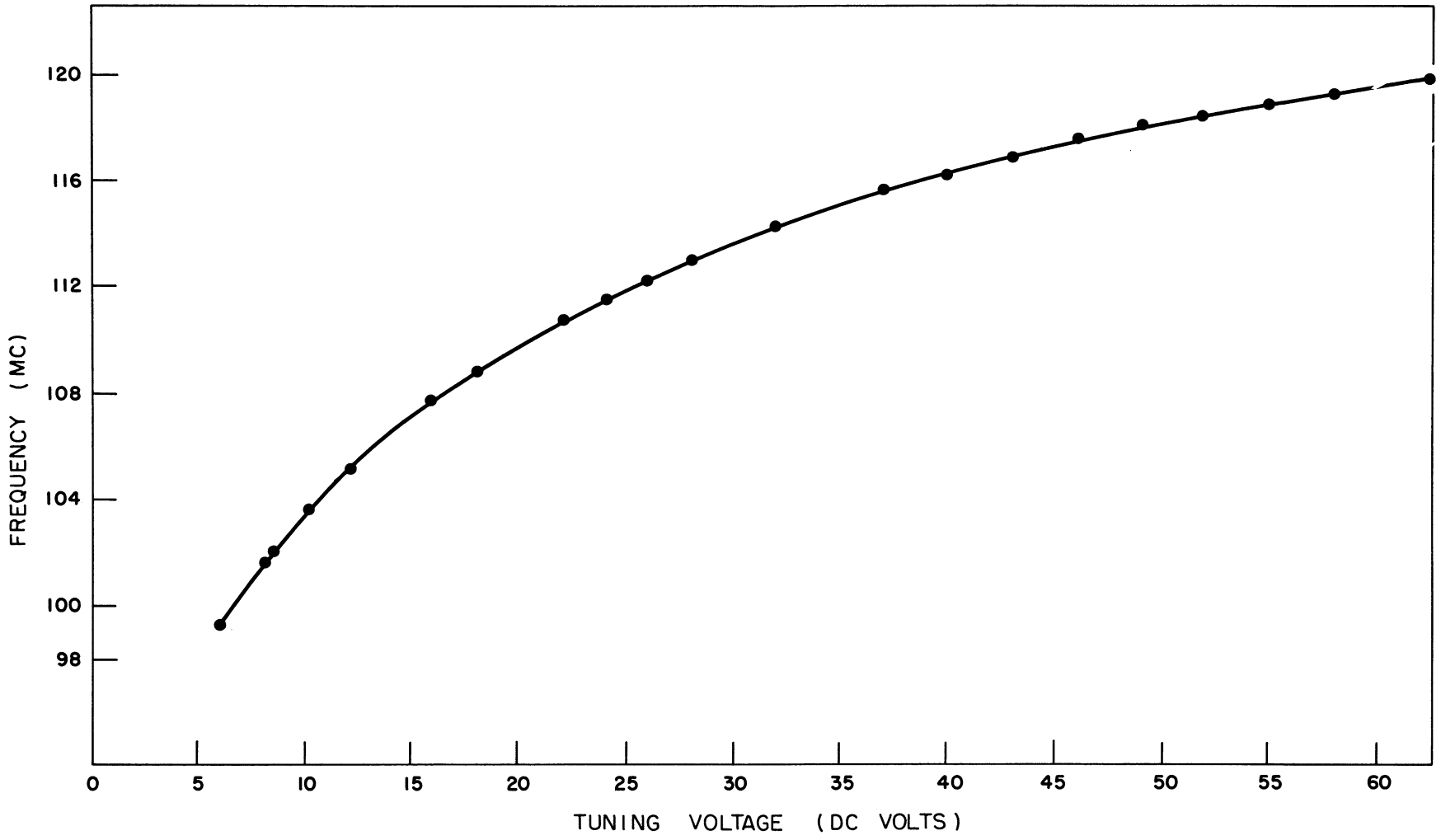

Fig. 14. High-frequency oscillator tuning curve.

stage for each is employed to obtain the 50-ohm output impedance. The tuning curves for the two tunable oscillators are given in Figs. 13 and 14.

The master crystal oscillator block consists of a 100-kc crystal-stabilized oscillator followed by an appropriate shaping circuit. The shaping circuit produces a trigger pulse for a blocking oscillator. The output of the blocking oscillator is a periodic pulse train with a period of 10 microseconds and a pulse duration of approximately 0.05 microsecond. The Fourier amplitude spectrum of this pulse train consists of uniformally spaced (every 100 kc) components with a $\frac{\sin x}{x}$ envelope. The first zero of this spectrum as determined with a spectrum analyzer is about 27 Mc. It is possible to change this zero by varying the blocking bias voltage (-11 volts dc was experimentally determined to be optimum). The pulse train is finally applied to two band-pass filters. One of these filters is a high-Q parallel resonant circuit tuned to 2 Mc. This provides a synchronization signal for the high-frequency discrete-frequency generator. The output of the second filter is the discrete-frequency reference signal. Figure 15(a) shows the time waveform of the first output, while 15(b) gives the frequency spectrum of the second.

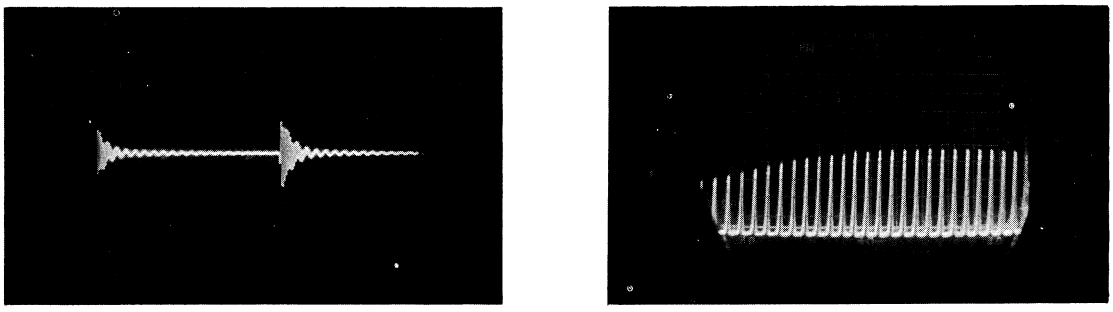

(a) (b)

Fig. 15. Master oscillator output waveform. (a) Time waveform of first output; (b) Frequency spectrum of second output.

The remaining two blocks to be considered are the discrete frequency generators. As explained above, the second output of the master oscillator supplies reference signals for the intermediate (second) frequency generator. When this reference is connected to the generator block it is first amplified by a voltage-tuned (the same voltage that is supplied to the oscillator) stage to provide greater selectivity of the desired harmonic. This amplified reference is then applied to a balanced mixer circuit along with the local oscillator signal. The balance mixer is the phase detector shown in Fig. 16. The output of the mixer plus the externally-supplied dc tuning voltage is further amplified and filtered by a dc amplifier. This resultant voltage is the one supplied to the local oscillator.

A very important aspect of the above block is the balanced mixer phase detector. A schemetic diagram of this type circuit is given in Fig. 16(a). The reference signal and local oscillator are supplied as shown. The transformer action supplies the linear sum and difference voltages of these two inputs, respectively, at the upper and lower diodes. The diodes perform as voltage multipliers and provide a dc output signal as shown in Fig. 16(b) if the oscillator and reference frequencies are identical. When there is a slight frequency difference between the two inputs, the mixer output is a low-frequency voltage which under proper conditions can cause the oscillator to lock to the reference frequency.

Finally, there is the high-frequency (first) discrete frequency generator. Here it is initially necessary to generate a precise 2-Mc clock pulse. This is done by phase-locking to the twentieth harmonic of the 100-kc oscillator provided from output "one" of the master oscillator; see Fig. 15(a). The two-megacycle clock pulse triggers a blocking oscil-

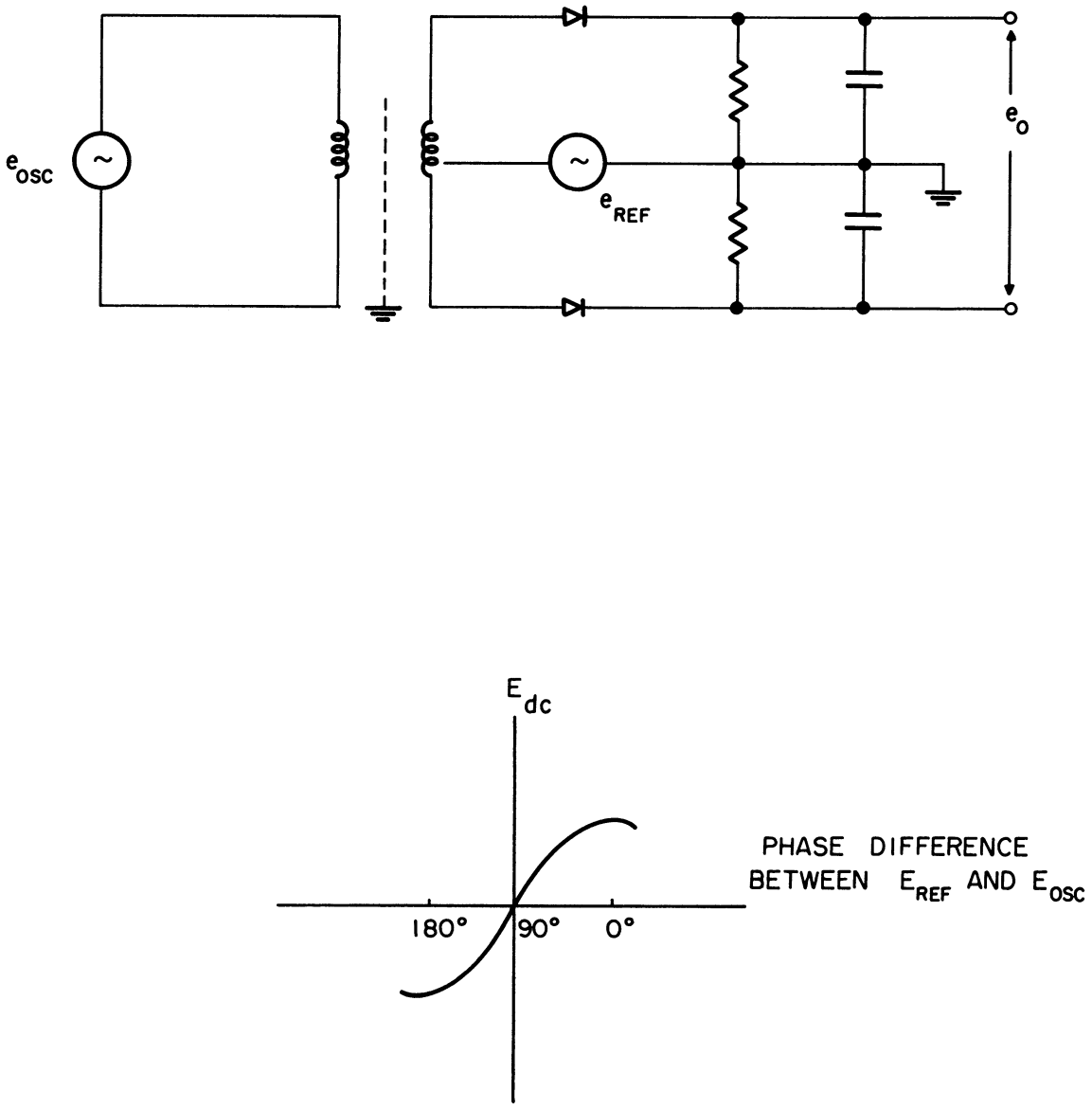

Fig. 16. Balanced-mixer phase detector.

lator to once again supply a discrete frequency reference. From this point on, the technique is identical to the intermediate unit described above. Naturally, the circuit implementation is more critical due to the higher frequency range. It was necessary to design and perfect a wide-band dc amplifier for the high-frequency phase-lock loop circuit to provide up to 1 Mc bandwidth (Ref. 2). Furthermore, a two-stage voltage-tuned amplifier was prepared to obtain a sufficient (50-mv) reference signal at the phase detector.

3.4 Performance and Evaluation

This section presents the results from a detailed determination of the receiver subsystem performance. Included also is an objective evaluation of the receiver concept based on the knowledge obtained in designing and building the system.

The first aspect of performance described pertains to the traditional receiver parameters. Table I lists the experimentally obtained midband

	1st Converter	2nd Converter	Detection Section	
			FM	AM
1. Tuning Range	80-102 Mc	18.0-20.0 Mc	4.5 Mc	4.5-4.6 Mc
2. Bandwidth	2.1 Mc	110 kc	100 kc	25 kc
3. Image Rejection	75 db	73 db	-	70 db
4. Sensitivity	0.5 uv	0.5 uv	-	50 uv
5. Conversion Gain	64 db	87 db	-	-
6. Dynamic Range	79 db	87 db	-	-
7. Noise Figure	8.5 db	-	-	-
8. Frequency Stability	Crystal Controlled (Better than five parts in 10^6).			

Table I. Receiver performance.

characteristics. It is noted that all design specifications were realized except for the full 80 db of image rejection. Items 2-7 of the Table I are subject to variation as a function of frequency, which in turn is determined by the tuning voltage.[1] This is primarily a consequence of the tuning-diode Q variation with voltage. Typically the performance is worse for the lower portion of the frequency range and better for the higher frequencies.

The second area of performance pertains to frequency stability. The entire receiver is tuned to certain harmonics of the master crystal oscillator. This oscillator operates at a frequency of 100 kc, and it was experimentally found to have a stability better than 5 parts in 10^6. It must be pointed out, however, that there is no provision for temperature stabilization of the crystal. With reasonable care a stability of 1 part in 10^8 should not be difficult to maintain with modern ovens and crystals if this were a system requirement.

When the receiver subsystem is phase-locked, then the receiver set-on accuracy is precisely the same as the stability of the master crystal oscillator. In the case of the experimental receiver this means that any discrete tuning point is obtained with a frequency accuracy of 5 parts in 10^6, or approximately $\pm$ 500 cps at 100 Mc. With a better crystal this could readily be reduced to $\pm$ 1 cycle at 100 Mc, which is certainly satisfactory for narrowband SSB communication receivers.

The experimentally obtained switching time from any given discrete frequency to any other is on the order of 20 microseconds. The limitation on this time is related to the bandwidth of the phase-lock loop in the second converter. If, for example, a tuning requirement of 10-kc

[1] Graphs indicating the tuning characteristics of the three voltage-tuned oscillators are given in Figs. 12, 13, and 14.

steps were imposed, then a third converter would be required, with a resulting switching time of about 200 microseconds. Thus, switching rate is traded for more closely spaced discrete tuning points. It is to be emphasized here that if one desires to make use of the rapid switching capability of a receiver of this type it is necessary to design the tuning voltage drive circuits carefully, to accomodate the switching rate. Furthermore, if the receiver is to be operated at a remote location, a control link of compatible bandwidth is also required.

The experience gained from developing the experimental receiver has provided some insight into designing a superior system. One of the most objectionable aspects of the present receiver is the need for a 2-Mc oscillator which is related to the 100-kc master oscillator. This is accomplished by locking a 2-Mc oscillator to the 20th harmonic of the master signal. Even by this technique (as contrasted with traditional multipliers) some 100-kc signals manage to slightly frequency-modulate the 2-Mc signal. This results in some small, but noticeable, spurious comb components in the output of the 1st discrete-frequency generator. These can currently be held 50 db below the major 2-Mc components; however, their presence is a shortcoming of the system. No similar problem exists in the 2nd DFG.

In an improved design it would be desirable to use directly a 2-Mc crystal and employ a divider circuit to supply the 100-kc comb. This would eliminate the spurious-component problem. Furthermore, a 2-Mc crystal is relatively small, an important consideration from the packaging point of view.

Two other problems encountered in constructing this receiver still fall in the "not-completely-solved" category. These are the develoments of a wide bandwidth phase-lock oscillator and the determination of an

optimum comb generator.

The first of these, the PLO work, has progressed to a point where 1-Mc-wide loops can be built as low as 10 Mc center frequency. The remaining major problem is an investigation of the optimum filter design for multi-component reference combs.[1]

The problem in comb generation can be simply stated. An ideal comb will have a maximum of energy uniformly distributed in the band of interest and have a voltage waveform with a minimum peak-to-average power ratio. To date, the ideal comb waveform is not known. A number of techniques for providing combs have been proposed, and two are currently in use. These are the blocking oscillator and the linear maximal shift-register generator. Both produce a $\frac{\sin x}{x}$ frequency distribution, but the shift-register has a 2n average power advantage over the blocking oscillator for equal peak powers. Here, n is the number of stages in the register. The circuit complexity, however, of even a 3- or 4-stage register is vastly more complex than a blocking oscillator.

4. TELEMETRY SUBSYSTEM

The telemetering subsystem for the Remote DF Receiver consists of two radio data links: a command link and a data link. Both of these are in the standard 216-220 Mc telemetry band. The command link consists of five FM subcarrier channels in the range 14.5-70 kc, together with a speech channel in the 50-5000 cps range. The data link consists of two subcarrier channels in the range 14.5-70 kc and a speech channel in the range 50-5000 cps. The channel frequency allocations are such that both radio links carry all seven subcarrier channels and the speech channel

---

[1] For a more detailed discussion of both of these problems see CEL TR-120 (Ref. 1).

simultaneously, allowing both command and data links to be monitored at either the remote or the base stations. A block diagram of the telemetry system is given in Fig. 17.

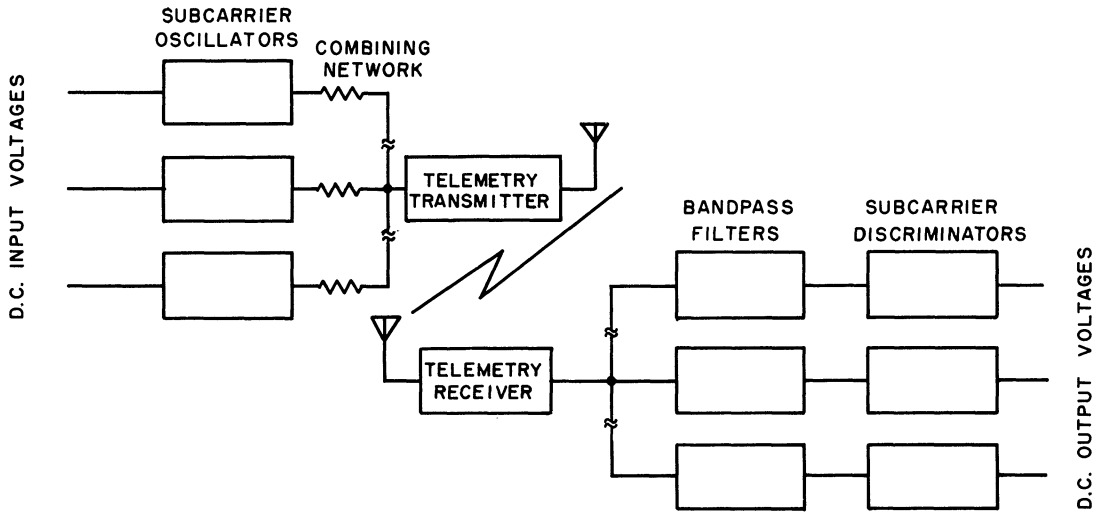

Fig. 17. Telemetry system.

The subcarrier oscillators and detectors were laboratory constructed along conventional lines. The subcarrier oscillators consist of an oscillator which is frequency-controlled by a ferroelectric voltage-variable capacitor. The subcarrier detectors are frequency discriminators consisting of a band-pass filter, amplitude limiter, heterodyne mixer, and integrative frequency counter. In order to minimize error, the local oscillators used in all the discriminators are synchronized to a master clock oscillator of high accuracy.

The radio links consist of surplus 20-watt, crystal-controlled, phase-modulated transmitters in the 220-megacycle range. Receivers are modified FM broadcast receivers; the antennas used with the links are

16-element yagis. The system is capable of transmitting tuning and control voltages from the control point to the remote receiver; and antenna bearing, received audio, and received signal level from the receiver to the control point; all with an accuracy of two percent.

4.1 Radio Links

Each of the two radio links consists of a 2-watt, 220-megacycle, phase-modulated transmitter followed by a 20-watt power amplifier. The transmitter and power amplifier are commercial equipment manufactured by Tele-Dynamics, Inc. The receivers are 88-megacycle broadcast FM receivers manufactured by Heath Company. A 220 megacycle-88 megacycle converter was laboratory constructed and is an integral part of these receivers.

The command link and data link are separated about a megacycle in transmitter frequency to prevent crosstalk between channels.

4.2 Subcarrier Equipment

The subcarrier equipment consists of a subcarrier oscillator and a subcarrier discriminator for each of seven channels. Five of these channels are reserved for tuning voltages to be transmitted from the control point to the remote receiver, while the remaining two are used for received signal strength and antenna bearing information to be transmitted from the receiver to the control point. The subcarrier equipment follows standard FM-FM telemetering standards promulgated by the IRITWG[1] regarding center frequency and deviation.

4.3 Subcarrier Oscillator

The subcarrier oscillator, diagrammed in Fig. 18, consists of a frequency-modulated Hartley oscillator followed by a buffer-amplifier. Input dc signals are amplified by a dc amplifier and applied to a pair of ferroelectric capacitors to accomplish the frequency modulation. As these

[1]Inter-Range Instrumentation and Telemetry Working Group.

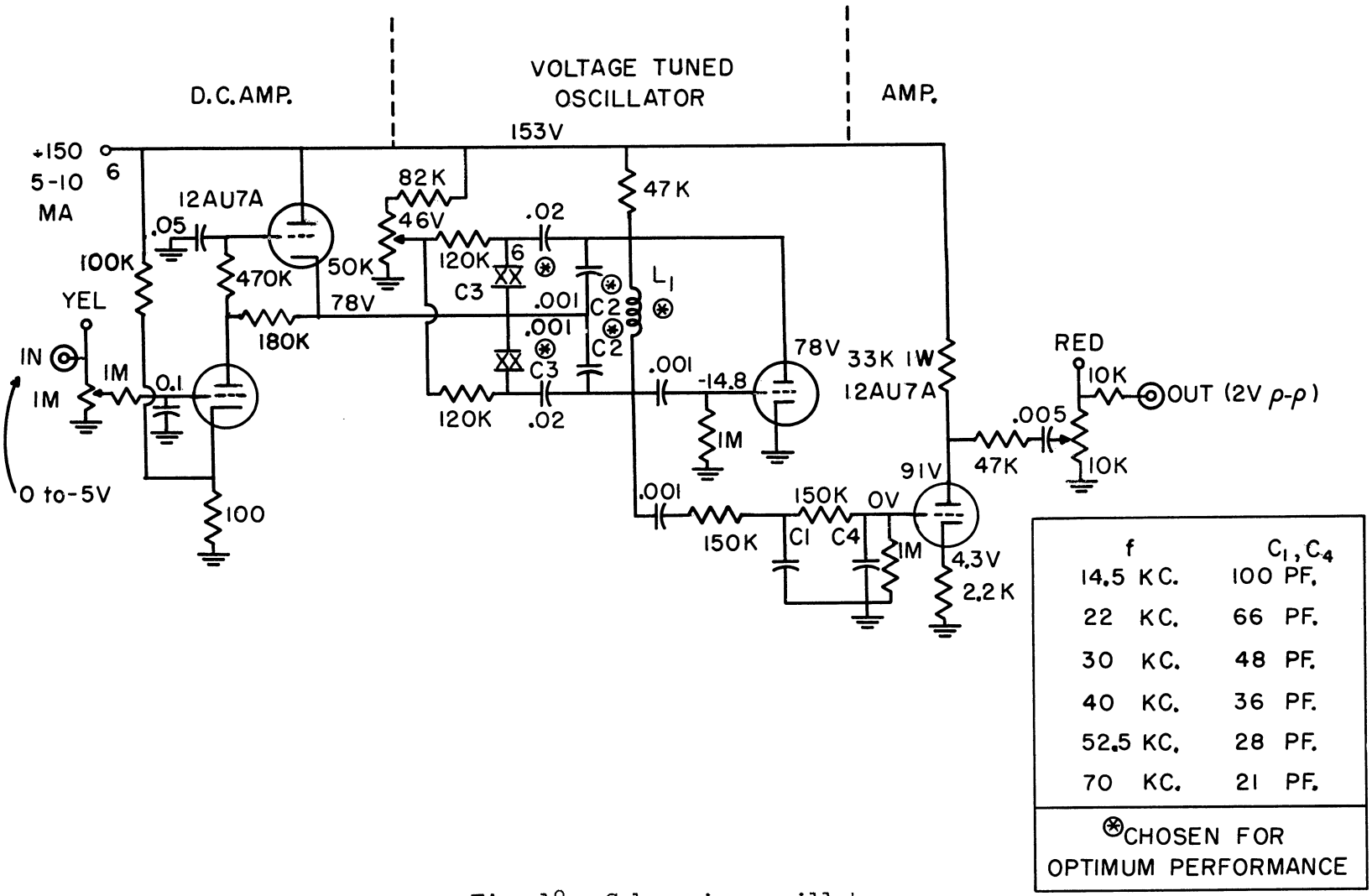

f	C_1, C_4
14.5 KC.	100 PF.
22 KC.	66 PF.
30 KC.	48 PF.
40 KC.	36 PF.
52.5 KC.	28 PF.
70 KC.	21 PF.

⊛CHOSEN FOR OPTIMUM PERFORMANCE

Fig. 18. Subcarrier oscillator.

capacitors are quite temperature sensitive, they are enclosed in a crystal-type oven maintained at 45°C.

4.4 Subcarrier Discriminators

The subcarrier discriminators are diagrammed in Fig. 19. They consist of a band-pass filter, which eliminates all frequencies but the desired channel, an amplitude limiter which removes amplitude variations of the desired channel signal, a mixer, a local oscillator, a low-pass filter, and a frequency counter. The combination of mixer, local oscillator, and low-pass filter effectively shifts the channel frequency to a lower one in the one- to ten-kilocycle range. The signal which varied from 31 to 33 kilocycles, for example, now varies from one to three. The frequency counter consists of a Schmidt trigger, which generates a square-wave pulse at constant amplitude, and an integrative-type diode detector which converts the pulse train into an analog voltage.

5. ANTENNA AND DISPLAY SUBSYSTEMS

5.1 Antenna Subsystem

The antenna subsystem consists of a horizontally polarized Adcock antenna with elements five feet in length. It was designed to rotate at speeds up to 250 rpm. A Sage Laboratories rotating RF joint is used to couple the rotating antenna to a 50-ohm coaxial cable and ultimately to the DF receiver. A rack mounted motor control unit was built for the antenna (see Fig. 20); a typical field pattern obtained from the Adcock antenna with a field-strength meter is shown in Fig. 21.

5.2 Display Subsystem

No elaborate unit was assembled for display purposes. The scheme consisted of feeding the detected audio signal from the DF receiver to the

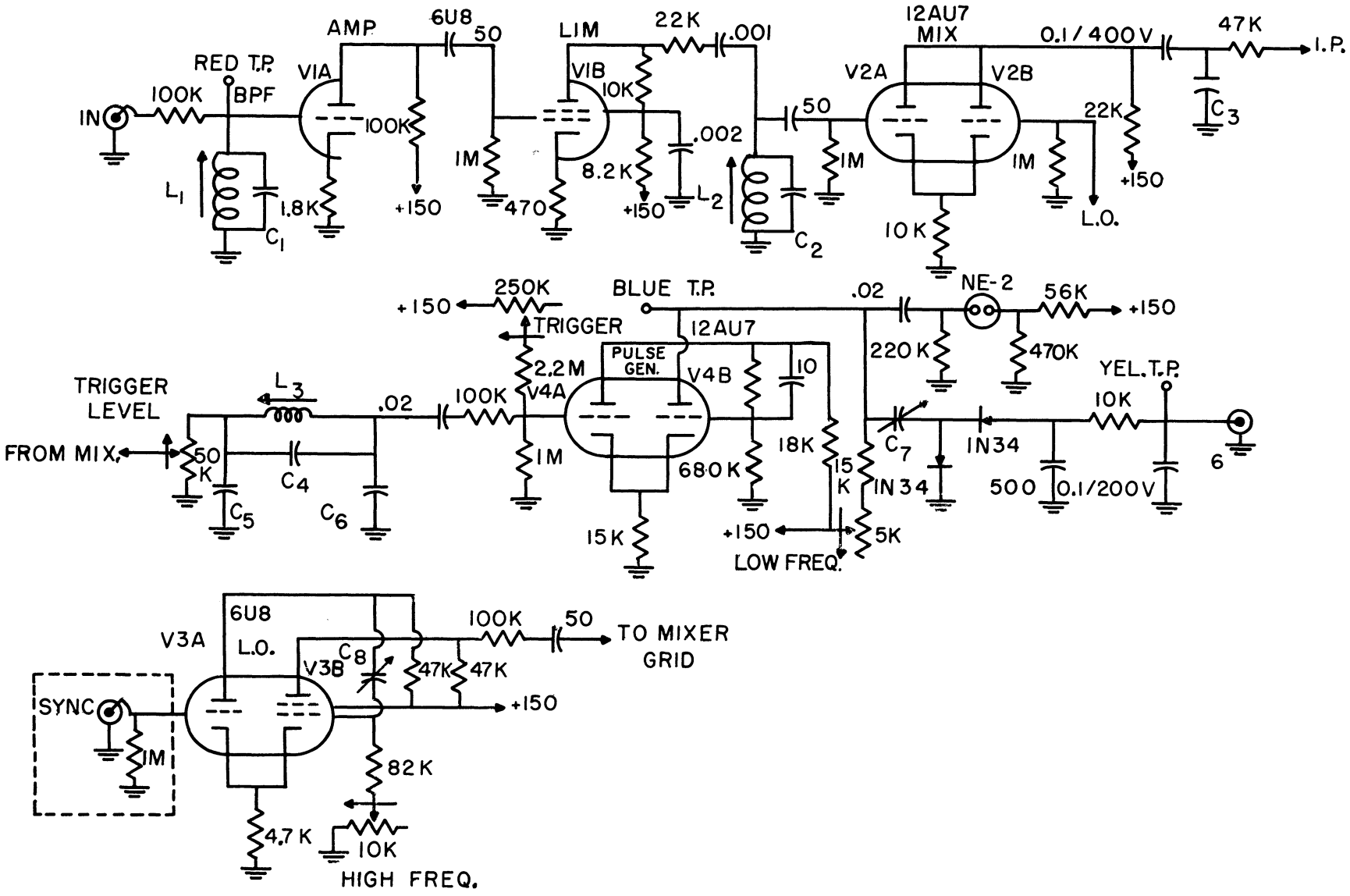

Fig. 19. Subcarrier discriminator.

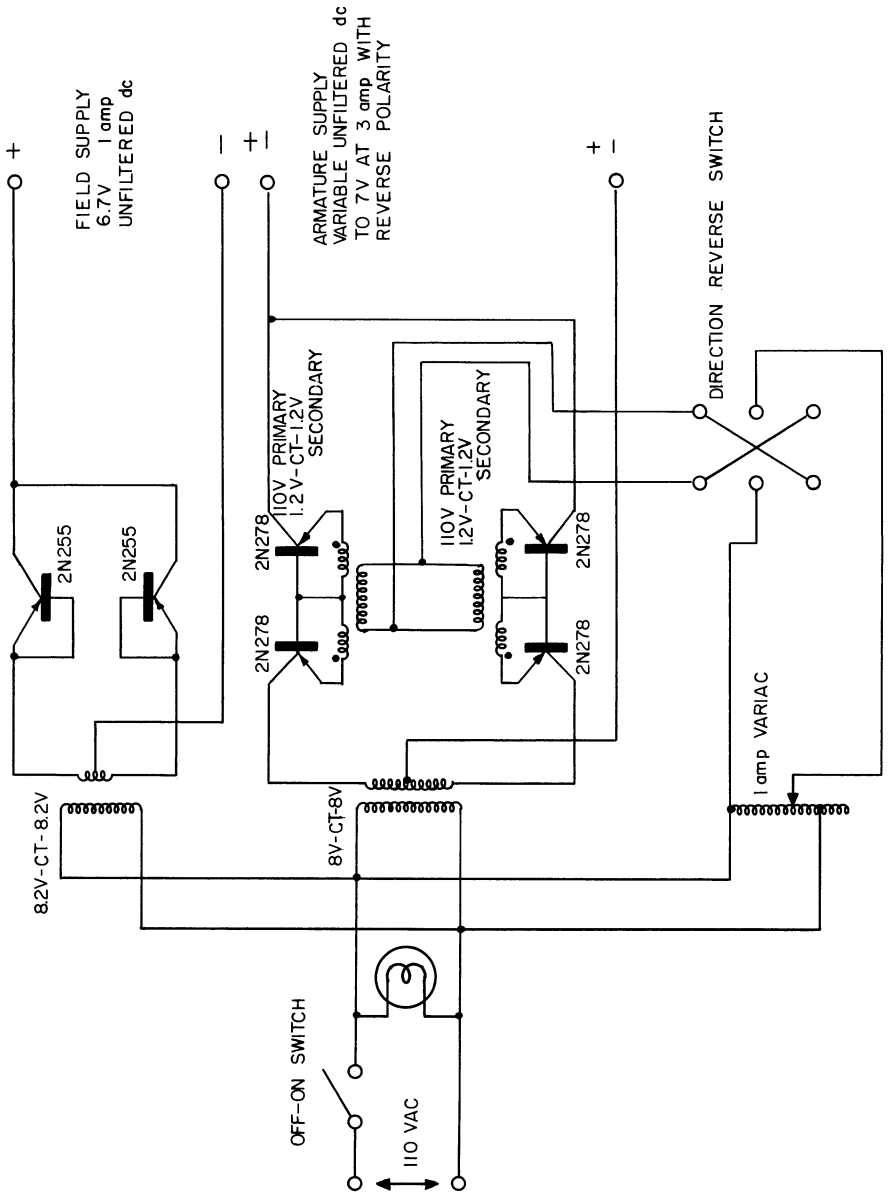

Fig. 20. Motor control unit.

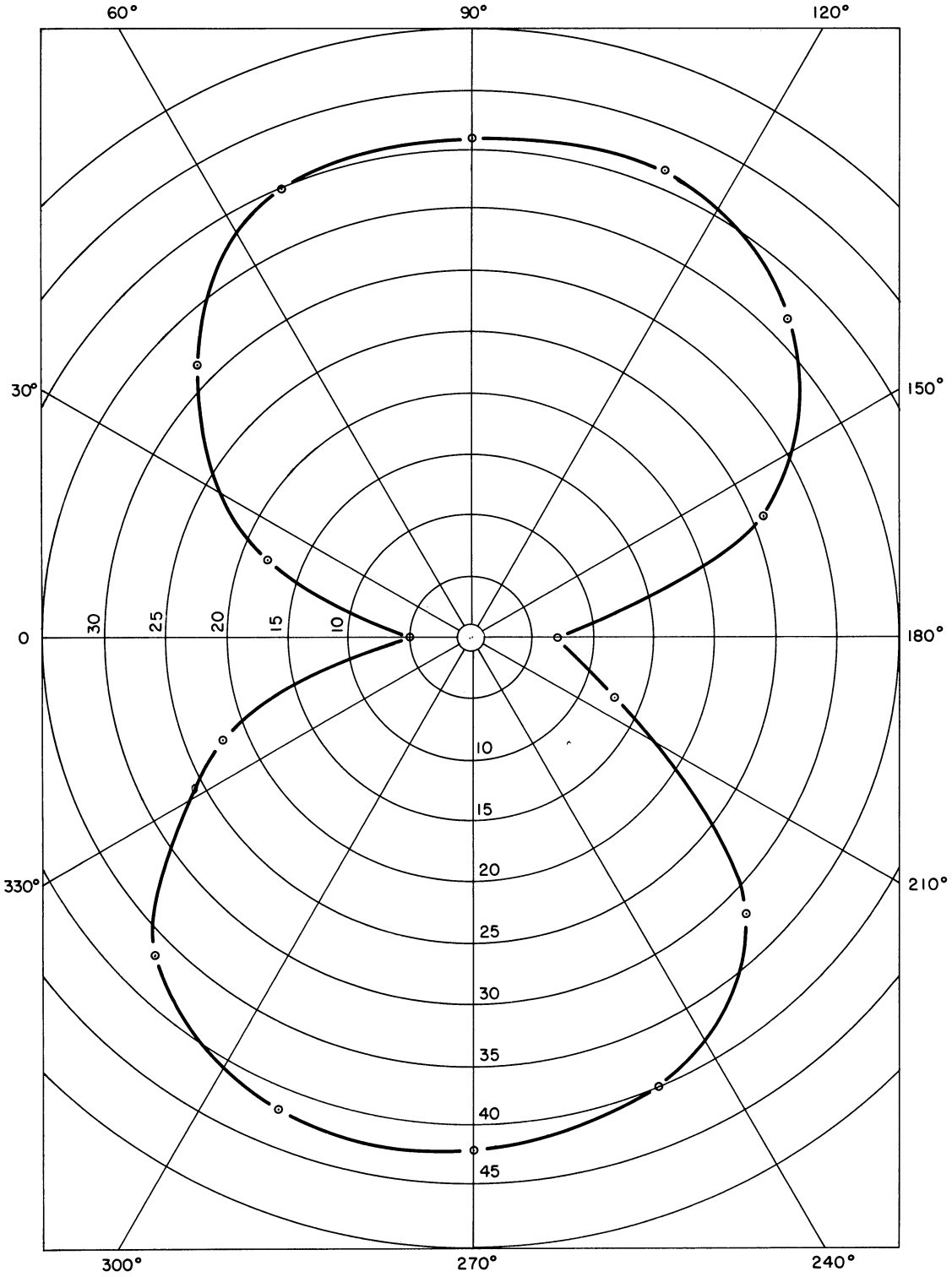

Fig. 21. Typical field pattern obtained from the Adcock antenna with a field-strength meter.

vertical plates of an oscilloscope. The sweeps were triggered as the antenna passed through north, and marker pips were inserted to indicate the cardinal directions of the DF antenna.

6. CONCLUSION

The initial objective of work described in this report was to demonstrate the feasibility of a Remotely-Controlled Tactical Direction-Finding System employing solid-state tuning devices. The major part of the effort on this project was expended on the development of the receiver system. One complete, rack-mounted, experimental receiver was built with an 80-102 Mc tuning range.

The receiver described in this report utilizes a discrete local oscillator to obtain both rapid frequency selection and precise tuning, two important requirements in DF equipment. These features are obtained at the expense of continuous tuning by providing a self-stored, crystal-controlled, discrete reference signal. Tuning of the receiver is accomplished by supplying two or three dc voltages or appropriate ac signals to generate the required dc voltages.

The principle result of this work was the design concept and construction of a specialized receiver. A number of practical applications for this receiver are listed in the introduction. Finally, the authors wish to emphasize the fact that the discrete tuning principle may be applied to other devices than receivers. Two such applications are:

1) A variable oscillator for transmitter applications.

2) A generalized frequency synthesizer.

Since the feasibility of this system has been adequately demonstrated further development of this and related systems should be considered.

APPENDIX A

PHASE-LOCK OSCILLATOR ANALYSIS

The typical phase-lock oscillator (PLO) configuration is depicted in Fig. 22(a). This circuit consists of a phase detector, a low-pass filter (or amplifier), and a voltage-controlled oscillator (VCO). For the following analysis it is convenient to consider the mathematical model depicted in Fig. 22(b) as a representation of the physical circuit. In this model the approximate tuning voltage is designated by V_t and the reference signal is assumed given by $V_r \cos [\omega t + \theta]$. The phase detector is shown as a multiplier while the VCO is symbolized as an integrater. By definition h(t) is the impulse response of the low-pass filter.

One aspect of the above model that frequently causes question is the portrayal of the VCO as an integrater. To explain this point it is necessary to examine the oscillator in greater detail. Consider, for example, the input control voltage to be

$$v_c(t) = V_t + V_c \sin \omega_c t \tag{1}$$

This voltage is applied to a voltage variable capacitor with the result that the effective circuit capacitance is

$$C [v_c(t)] = C [V_t + V_c \sin \omega_c t] \tag{2}$$

The capacitance C is not a linear function of voltage, however, for practical purposes when $V_c \ll V_t$ the truncated Taylor's series expansion yields

$$C [v_c(t)] \cong C (V_t) + \left.\frac{dC}{dv}\right|_{v=V_t} V_c \sin \omega_c t \tag{3}$$

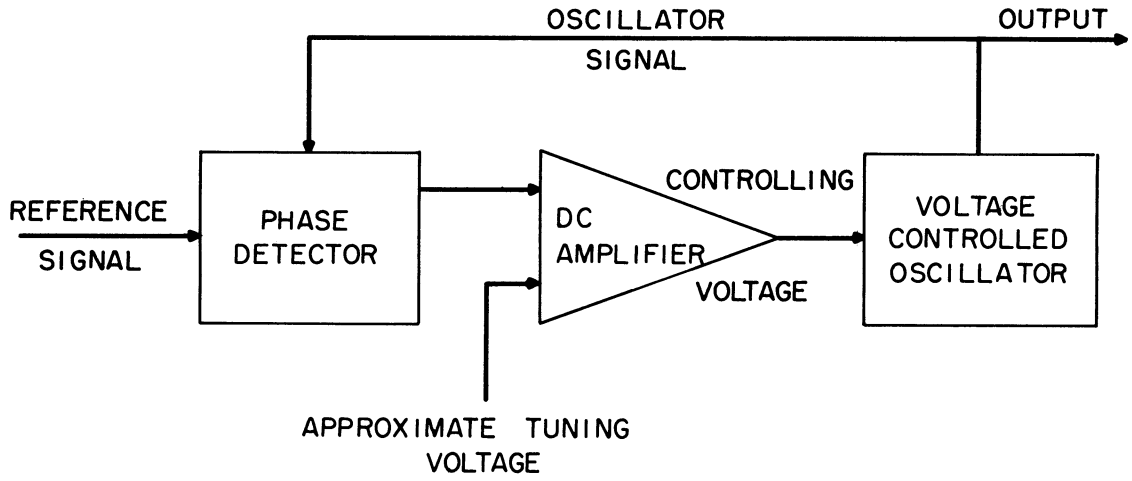

(a) Physical circuit.

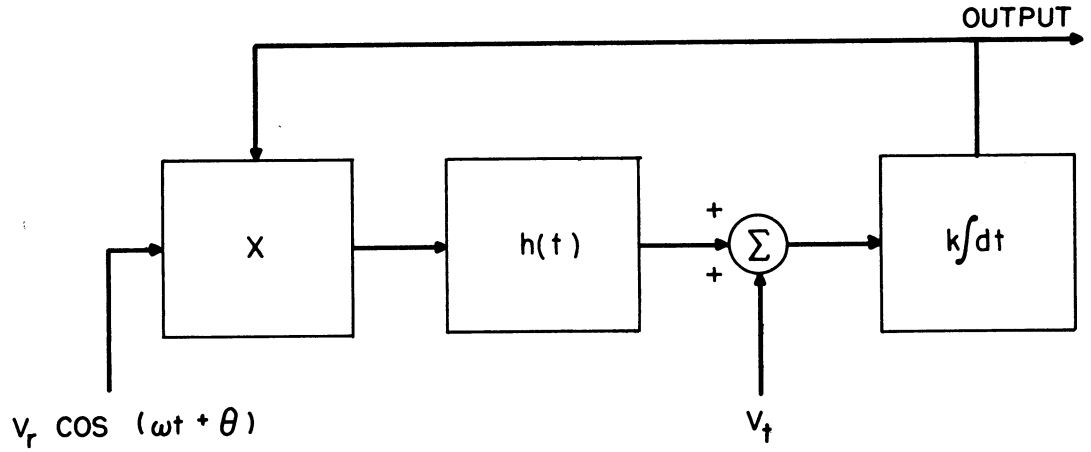

(b) Mathematical model.

Fig. 22. Phase-lock oscillator configuration.

a good approximation. It follows that the frequency of the oscillator is given approximately by

$$f(t) = \frac{1}{2\pi \sqrt{LC[v_c(t)]}} = \frac{1}{2\pi \sqrt{LC(V_t) + L \frac{dC}{dv}\Big|_{v=V_t} V_c \sin \omega_c t}} \quad (4)$$

If f_t is defined by

$$f_t = \frac{1}{2\pi \sqrt{LC(V_t)}} \quad (5)$$

then

$$f(t) = \frac{f_t}{\sqrt{1 + \frac{V_c}{C(V_t)} \frac{dC}{dv}\Big|_{v=V_t} \sin \omega_c t}} \quad (6)$$

Typically

$$\frac{V_c}{C(V_t)} \frac{dC}{dv}\Big|_{v=V_t} \ll 1$$

Hence, as an approximation

$$f(t) \cong f_t (1 - \alpha \sin \omega_c t) \quad (7)$$

where by definition

$$\alpha = \frac{V_c}{2\, C(V_t)} \frac{dC}{dv}\Big|_{v=V_t}$$

The last equation describes the time varying frequency (FM) resulting from the applied voltage, $v_c(t)$. The oscillator phase, $\varphi(t)$, is obtained

by integrating the frequency

$$\varphi(t) = 2\pi \int_o^t f(\tau)\, d\tau + \varphi_o \tag{8}$$

or

$$\varphi(t) = 2\pi \left(f_t t + \frac{\alpha f_t}{\omega_c} \cos \omega_c t \right) + \varphi_o \tag{9}$$

$$= \omega_t t + \frac{\alpha f_t}{f_c} \cos \omega_c t + \varphi_o \tag{10}$$

where $\omega_t = 2\pi f_t$. Equation (10) is the traditional expression for the phase of a sinusoidally modulated FM signal with a frequency deviation of αf_t . It follows from Eqs. (1) and (9) that the VCO phase is the time integral of the tuning voltage times some appropriate constant, k. The value of k is solely a function of tuning bias and can be either experimentally or analytically determined. k is given by

$$k = - \frac{2\pi f_c \left. \frac{dC}{dv} \right|_{v=V_t}}{2\, C(V_t)} = - \frac{\left. \frac{dC}{dv} \right|_{v=V_t}}{2\, C(V_t)\, \sqrt{LC(V_t)}} \tag{11}$$

Since $\frac{dC}{dv}$ is negative, k has a positive value. Thus the VCO actually serves as an ideal integrator as shown in the block diagram, Fig. A-1(b).

The next step is to obtain the differential equation describing the phase-lock oscillator. With reference to Fig. A-1(b), it is seen that the multiplier output is given by

$$v_c'(t) = k' V_r V_o \sin \varphi(t) \cos [\omega t + \theta] \tag{12}$$

which can be expressed as

$$v_c'(t) = \frac{k' V_r V_o}{2} \left\{ \sin [\varphi(t) + \omega t + \theta] + \sin [\varphi(t) - \omega t - \theta] \right\} \tag{13}$$

where k' is the conversion gain or loss associated with the multiplier and has dimensions, $(\text{voltage})^{-1}$. To simplify the following equations, it is convenient to define

$$V_c = \frac{k' V_r V_o}{2} = \text{magnitude of the error signal}$$

and

$$\psi(t) = \varphi(t) - \omega t - \theta = \text{instantaneous phase error.}$$

Thus equation (13) may be written as

$$v_c'(t) = V_c \left\{ \sin [\psi(t) + 2\omega t + 2\theta] + \sin \psi(t) \right\} \qquad (14)$$

It will be assumed here that the first term on the right side of equation (14) will be completely attenuated by the low-pass filter. Consequently, the voltage, $v_c(t)$, is given by

$$v_c(t) = V_t + V_c \sin \psi(t) * h(t) \qquad (15)$$

The effect of the control voltage $v_c(t)$ has already been described. Starting with $v_c(t)$ as defined in Eq. (15) and paralleling the development of Eqs. (1) - (9), the expression for frequency, corresponding to Eq. 7, becomes,

$$f(t) = f_t [1 - \alpha \sin \psi(t) * h(t)] \qquad (16)$$

and hence the oscillator phase is given by

$$\varphi(t) = 2\pi f_t [t - \alpha \int_o^t \sin \psi(\tau) * h(\tau)\, d\tau] + \varphi_o$$

$$= \omega_t t - \Delta\omega \int_o^t \sin \psi(\tau) * h(\tau)\, d\tau + \varphi_o \qquad (17)$$

where, $\Delta\omega = 2\pi f_t \alpha$. Thus, substituting for $\varphi(t)$

$$\psi(t) = (\omega_t - \omega)\, t - \Delta\omega \int_o^t \sin \psi(\tau) * h(\tau)\, d\tau + (\varphi_o - \theta) \qquad (18)$$

or

$$\psi(t) = \bar{\omega} t - \Delta\omega \int_o^t \sin \psi(\tau) * h(\tau)\, d_\tau + \bar{\theta} \qquad (19)$$

where, $\bar{\omega} = \omega_t - \omega$ and $\bar{\theta} = \varphi_o - \theta$.

If Eq. (19) is differentiated with respect to t, the result is

$$\dot{\psi} = \omega - \Delta\omega \sin \psi(t) * h(t) \qquad (20)$$

and rearranging terms this becomes

$$\dot{\psi} + \Delta\omega \sin \psi(t) * h(t) = \bar{\omega} \qquad (21)$$

Equation (21) is the general differential equation describing the phase-lock oscillator with a sinusidal reference and any linear, constant coefficient filter network.

For realizable networks, Eq. (21) is expressed by

$$\dot{\psi} + \Delta\omega \int_o^t h(t - \tau) \sin \psi(\tau)\, d\tau = \bar{\omega} \qquad (22)$$

a second differentiation yields

$$\ddot{\psi}(t) + \Delta\omega\, h(0) \sin \psi(t) + \Delta\omega \int_o^t \frac{2\, h(t - \tau)}{2t} \sin \psi(\tau)\, d\tau = 0 \qquad (23)$$

Either Eq. (22) or (23) may be used to obtain the differential equation describing a particular system once an expression for h(t) is supplied.

Next, three examples will be presented to demonstrate one application of the above development. First consider the low-pass filter as a

simple RC network. In this case

$$h(t) = \frac{\exp(-t/RC)}{RC} \tag{24}$$

Substituting this function in Eq. (23) yields

$$\ddot{\psi} + \frac{\Delta\omega}{RC}\sin\psi - \frac{\Delta\omega}{(RC)^2}\int_0^t \exp\left[\frac{-(t-\tau)}{RC}\right]\sin\psi(\tau)\,d\tau = 0 \tag{25}$$

But from Eq. 22,

$$\frac{\Delta\omega}{(RC)^2}\int_0^t \exp\left[\frac{-(t-\tau)}{RC}\right]\sin\psi(\tau)\,d\tau = \frac{\bar{\omega} - \dot{\psi}}{RC} \tag{26}$$

Combining these last two equations gives

$$RC\,\ddot{\psi} + \dot{\psi} + \Delta\omega\sin\psi = \bar{\omega} \tag{27}$$

This is the simplest of the class differential equations describing PLO operation. More will be said about Eq. (27) in a later section.

For a second example, consider an impulse response of the form

$$h(t) = \frac{\tau_1}{\tau_2}\delta(t) + \frac{\tau_2 - \tau_1}{\tau_2^2}\exp\left[\frac{-t}{\tau_2}\right] \tag{28}$$

The corresponding transfer function is

$$Y(p) = \frac{1 + \tau_1 p}{1 + \tau_2 p} \tag{29}$$

These equations define an RC filter of the type frequently discussed in the literature for PLO applications. Substituting Eq. (28) in Eq. (22) yields

$$\dot{\psi} + \Delta\omega\frac{\tau_1}{\tau_2}\sin\psi(t) +$$

$$\Delta\omega\frac{(\tau_2 - \tau_1)}{\tau_2^2}\exp\left[\frac{-t}{\tau_2}\right]\int_0^t \exp\left[\frac{\tau}{\tau_2}\right]\sin\psi(\tau)\,d\tau = \bar{\omega} \tag{30}$$

Differentiating

$$\ddot{\psi} + \Delta\omega \frac{\tau_1}{\tau_2} \cos \psi \ \dot{\psi} - \Delta\omega \frac{(\tau_2 - \tau_1)}{\tau_2^3} \exp\left[\frac{-t}{\tau_2}\right] \int_o^t \exp\left[\frac{\tau}{\tau_2}\right] \sin \psi(\tau)\, d\tau +$$

$$\Delta\omega \frac{(\tau_2 - \tau_1)}{\tau_2^2} \sin \psi = 0 \qquad (31)$$

But from Eq. (30) it follows that

$$-\Delta\omega \frac{(\tau_2 - \tau_1)}{\tau_2^3} \exp\left[\frac{-t}{\tau_2}\right] \int_o^t \exp\left[\frac{\tau}{\tau_2}\right] \sin \psi(\tau)\, d\tau =$$

$$\frac{\dot{\psi}}{\tau_2} + \Delta\omega \frac{\tau_1}{\tau_2} + \Delta\omega \frac{\tau_1}{\tau_2^2} \sin\psi - \frac{\bar{\omega}}{\tau_2} \qquad (32)$$

Substituting this into Eq. (31)

$$\tau_2 \ddot{\psi} + (1 + \Delta\omega \tau_1 \cos \psi) \dot{\psi} + \Delta\omega \sin \psi = \bar{\omega} \qquad (33)$$

The advantage of Eq. (33) over Eq. (27) is the independent control over damping afforded by the term $\Delta\omega \tau_1 \cos\psi$.

As a final example, h(t) will be assumed to be

$$h(t) = k_o + \frac{1}{\tau} \exp\left[\frac{-t}{\tau}\right] \qquad (34)$$

which has a transfer function given by

$$Y(p) = \frac{k_o}{p} + \frac{1}{\tau_o}\left(\frac{1}{p + \frac{1}{\tau_o}}\right) = \frac{k_o\tau+1}{\tau_o}\left[\frac{p + \frac{k_o}{k_o\tau_o+1}}{p\,(p + \frac{1}{\tau_o})}\right] \qquad (35)$$

This impulse response yields a third order differential equation as can be demonstrated by substituting Eq. (34) into Eq. (22), with the result

$$\dot{\psi} + \Delta\omega \int_o^t k_o + \frac{1}{\tau_o} \exp\left[-\frac{(t-\tau)}{\tau_o}\right] \sin \dot{\psi}(\tau)\, d\tau = \bar{\omega} \qquad (36)$$

or

$$\dot{\psi} + k_o \Delta\omega \int_o^t \sin \psi(\tau)\, d\tau +$$

$$\frac{\Delta\omega}{\tau_o} \exp\left[-\frac{t}{\tau_o}\right] \int_o^t \exp\left[\frac{\tau}{\tau_o}\right] \sin \psi(\tau)\, d\tau = \bar{\omega} \tag{37}$$

Differentiating,

$$\ddot{\psi} + k_o \Delta\omega \sin\psi - \frac{\Delta\omega}{\tau_o^2} \exp\left[\frac{-t}{\tau_o}\right] \int_o^t \exp\left[\frac{\tau}{\tau_o}\right] \sin\psi(\tau)\, d\tau +$$

$$\frac{\Delta\omega}{\tau_o} \sin = 0 \tag{38}$$

or

$$\ddot{\psi} - \frac{\Delta\omega}{\tau_o^2} \exp\left[\frac{-t}{\tau_o}\right] \int_o^t \exp\left[\frac{\tau}{\tau_o}\right] \sin\psi(\tau)\, d\tau +$$

$$\Delta\omega \left(k_o + \frac{1}{\tau_o}\right) \sin\psi = 0 \tag{39}$$

From Eq. (37)

$$-\frac{\Delta\omega}{\tau_o^2} \exp\left[\frac{-t}{\tau_o}\right] \int_o^t \exp\left[\frac{\tau}{\tau_o}\right] \sin\psi(\tau)\, d\tau =$$

$$\frac{\dot{\psi}}{\tau_o} + \frac{k_o \Delta\omega}{\tau_o} \int_o^t \sin\psi(\tau)\, d\tau - \frac{\bar{\omega}}{\tau_o} \tag{40}$$

which if substituted into Eq. (39) yields

$$\ddot{\psi} + \frac{\dot{\psi}}{\tau_o} + \frac{k_o \Delta\omega}{\tau_o} \int_o^t \sin\psi(\tau)\, d\tau - \frac{\bar{\omega}}{\tau_o} +$$

$$\Delta\omega \left(k_o + \frac{1}{\tau_o}\right) \sin\psi = 0 \tag{41}$$

Differentiating again,

$$\dddot{\psi} + \frac{\ddot{\psi}}{\tau_o} + \Delta\omega \left(k_o + \frac{1}{\tau_o}\right) \cos \psi \quad \dot{\psi} + \frac{\Delta\omega \, k_o}{\tau_o} \sin \psi = 0 \qquad (42)$$

This, then is the differential equation for a PLO with integral feedback in addition to the simple RC filter.

The above three typical examples have been included to demonstrate the application of Eqs. (22) and (23) when an analysis of a PLO is required. Naturally, it is either necessary to solve these equations or extract from them the desired information to complete the analysis. This will be discussed briefly in the following paragraphs.

Consider again Eq. (27) which is repeated below

$$RC \ddot{\psi} + \dot{\psi} + \Delta\omega \sin \psi = \bar{\omega} \qquad (43)$$

It is frequently assumed in the liturature that the RC product is sufficiently small that Eq. (43) effectively reduces to

$$\dot{\psi} + \Delta\omega \sin \psi = \bar{\omega} \qquad (44)$$

This approximation is only reasonable when

$$RC \ll \frac{1}{4 \, \Delta\omega}$$

and even under this condition the character of the solution is markedly altered.

The singular points of Eq. (44) are given by setting $\dot{\psi} = 0$, or

$$\psi = \sin^{-1} \frac{\bar{\omega}}{\Delta\omega} \qquad (45)$$

These points are alternately stable or unstable as demonstrated in Fig. 23.

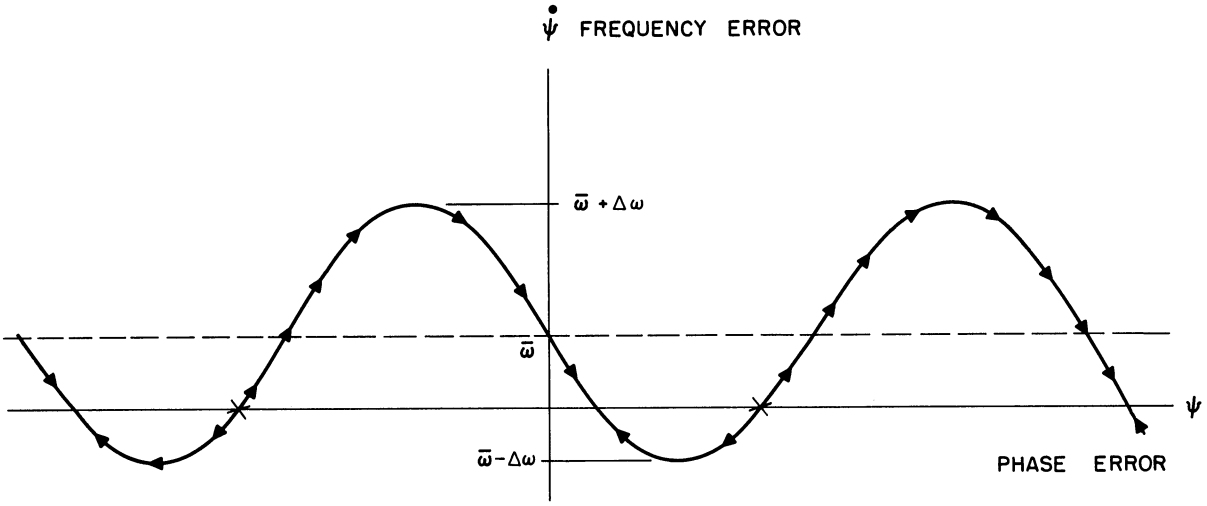

Fig. 23. Singular points of Eq. 44.

Since, by definition

$$\psi(t) = \varphi(t) - \omega t - \theta \tag{46}$$

the system will lock with

$$\dot{\psi}(t) = 0 = \dot{\varphi}(t) - \omega \tag{47}$$

or at a frequency

$$\dot{\varphi}_{lock} = \omega \tag{48}$$

and with a phase

$$\varphi_{lock} = \omega t + \theta + \sin^{-1}\left(\frac{\bar{\omega}}{\Delta\omega}\right) \tag{49}$$

It is to be observed that a necessary and sufficient condition for lock is

$$\bar{\omega} \leq \Delta\omega$$

If this condition is not satisfied the system will be in a state of periodic frequency oscillation.

Another factor of importance is the pull-in time of the PLO. This can be determined by writing Eq. (44) as

$$\frac{dt}{d\psi} = \frac{1}{\bar{\omega} - \Delta\omega \sin\psi} \tag{50}$$

and integrating yields a pull-in time, t

$$t = \int_{\psi_{\text{initial}}}^{\psi_{\text{lock}}} \frac{d\psi}{\bar{\omega} - \Delta\omega \sin\psi} \tag{51}$$

Since ψ_{lock} is given by $\sin^{-1}\frac{\bar{\omega}}{\Delta\omega}$, it is observed from Eq. (51) that the pull-in time will be infinite. This follows since the Lipschitz[1] condition is not violated at the singular point. To circumvent this problem it is possible to define a zero difference frequency time, t_{ZDF}, such that at t_{ZDF} a one-cycle difference frequency exists. This is determined by integrating the phase to ψ_{ZPF}, where

$$\psi_{ZDP} = \sin^{-1}\left(\frac{\bar{\omega} - 1}{\Delta\omega}\right) \tag{52}$$

or

$$t_{ZDF} = \int_{\psi_{\text{initial}}}^{\psi_{ZDF}} \frac{d\psi}{\bar{\omega} - \Delta\omega \sin\psi} \tag{53}$$

Evaluating this integral is somewhat involved; however, it can be shown

---

[1]The Lipschitz condition requires that

$\left|\bar{\omega} - \Delta\omega \sin\psi - \bar{\omega} + \Delta\omega \cdot \frac{\bar{\omega}}{\Delta\omega}\right| = \left|\bar{\omega} - \Delta\omega \sin\psi\right| \leq M \left|\psi - \sin^{-1}\frac{\bar{\omega}}{\Delta\omega}\right|$, where M is a positive constant.

that, (see TR-120)

$$t_{ZDF} \cong \frac{\ln 2\ \Delta\omega}{\Delta\omega} \tag{54}$$

where $\Delta\omega \gg \bar{\omega}$.

Now consider Eq. (43) directly, it may be put in the following form

$$\begin{aligned} \dot{\psi} &= \beta \\ \dot{\beta} &= \frac{\bar{\omega} - \Delta\omega \sin\psi - \beta}{RC} \end{aligned} \tag{55}$$

The singular points for this equation are given by the condition

$$\dot{\psi} = \dot{\beta} = 0$$

or

$$\psi = \sin^{-1} \frac{\bar{\omega}}{\Delta\omega} \tag{56}$$

which is exactly the same as in the previous case.

The phase plane for Eq. (55) is substantially different from the one depicted in Fig. 23 for Eq. (44). For example, the second-order equation has multiple solution paths as contrasted with the single path of Eq. (44). Furthermore, the effect of damping due to the term $\frac{\dot{\psi}}{RC}$ is placed very much in evidence.

A further discussion of Eqs. (33) and (42) will not be presented here. The interested reader is referred to TR-120 for more information on Eq. (33) and to Reference 3 for Eq. (42).

APPENDIX B

DETAILED CIRCUIT DIAGRAMS FOR THE RECEIVER SUBSYSTEM

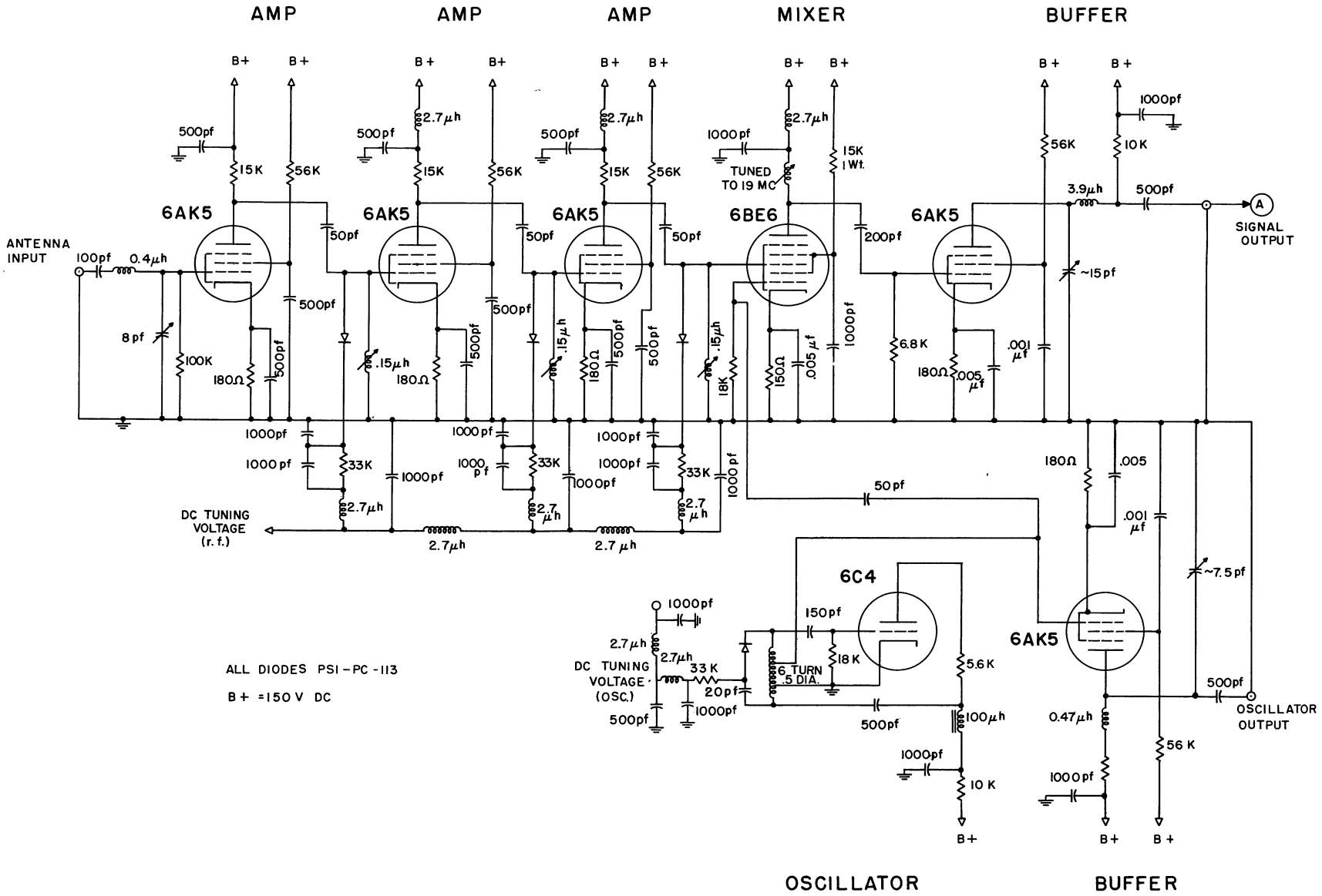

Fig. 24. First RF amplifier and mixer (80-102 Mc).

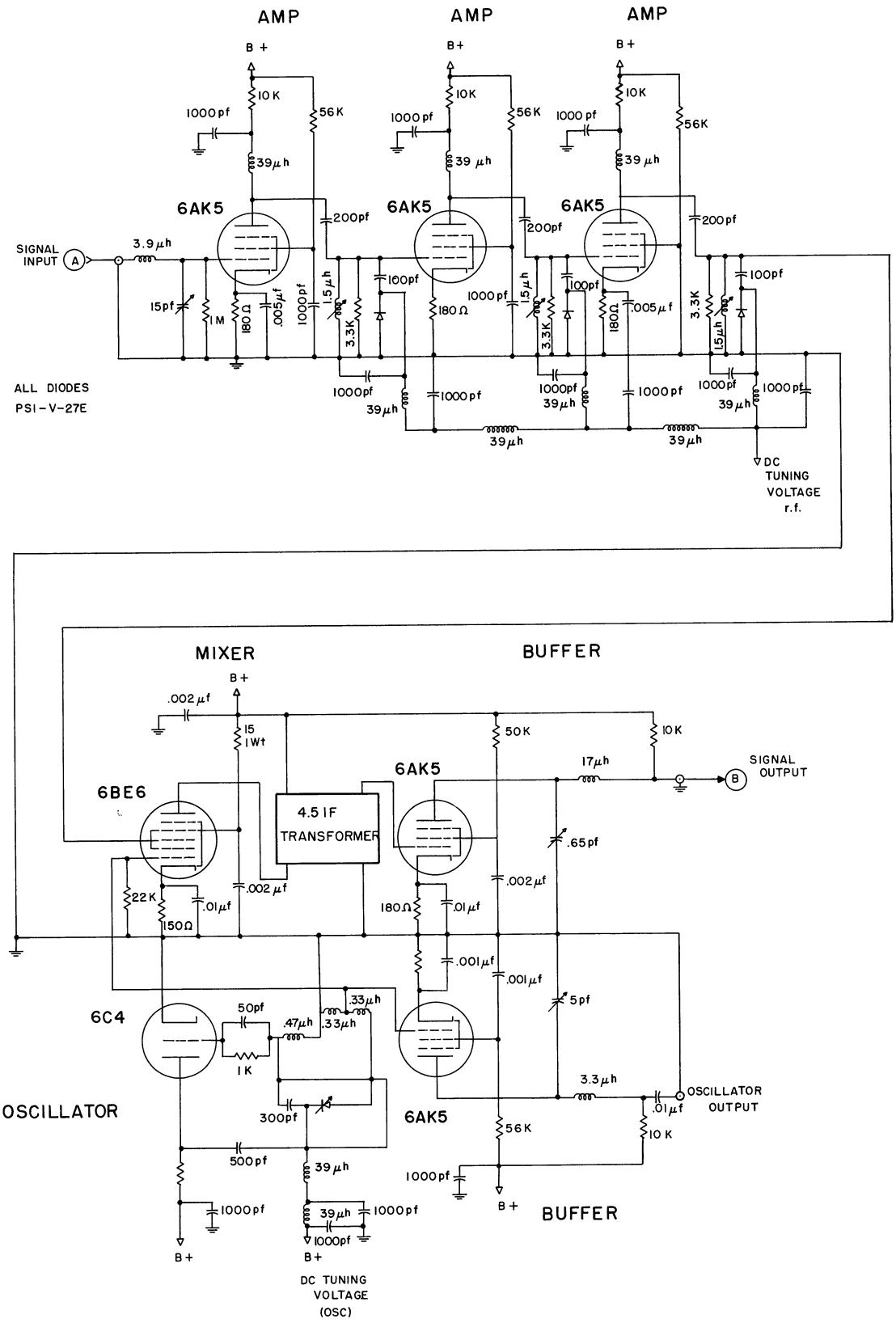

Fig. 25. Second RF amplifier and mixer (18.0-20.0 Mc).

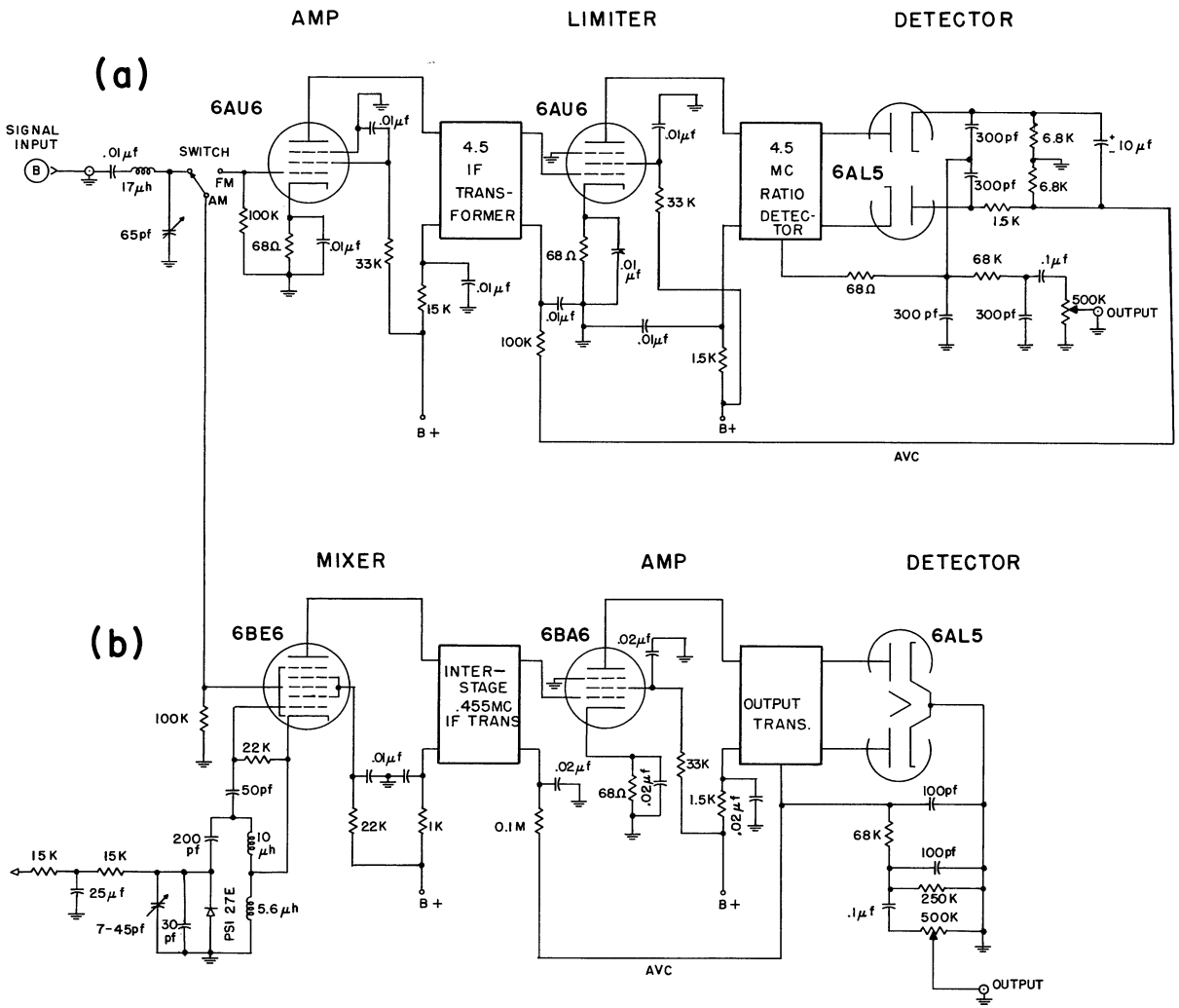

Fig. 26. (a) FM-IF and detector unit; (b) AM-mixer, IF, and detector units.

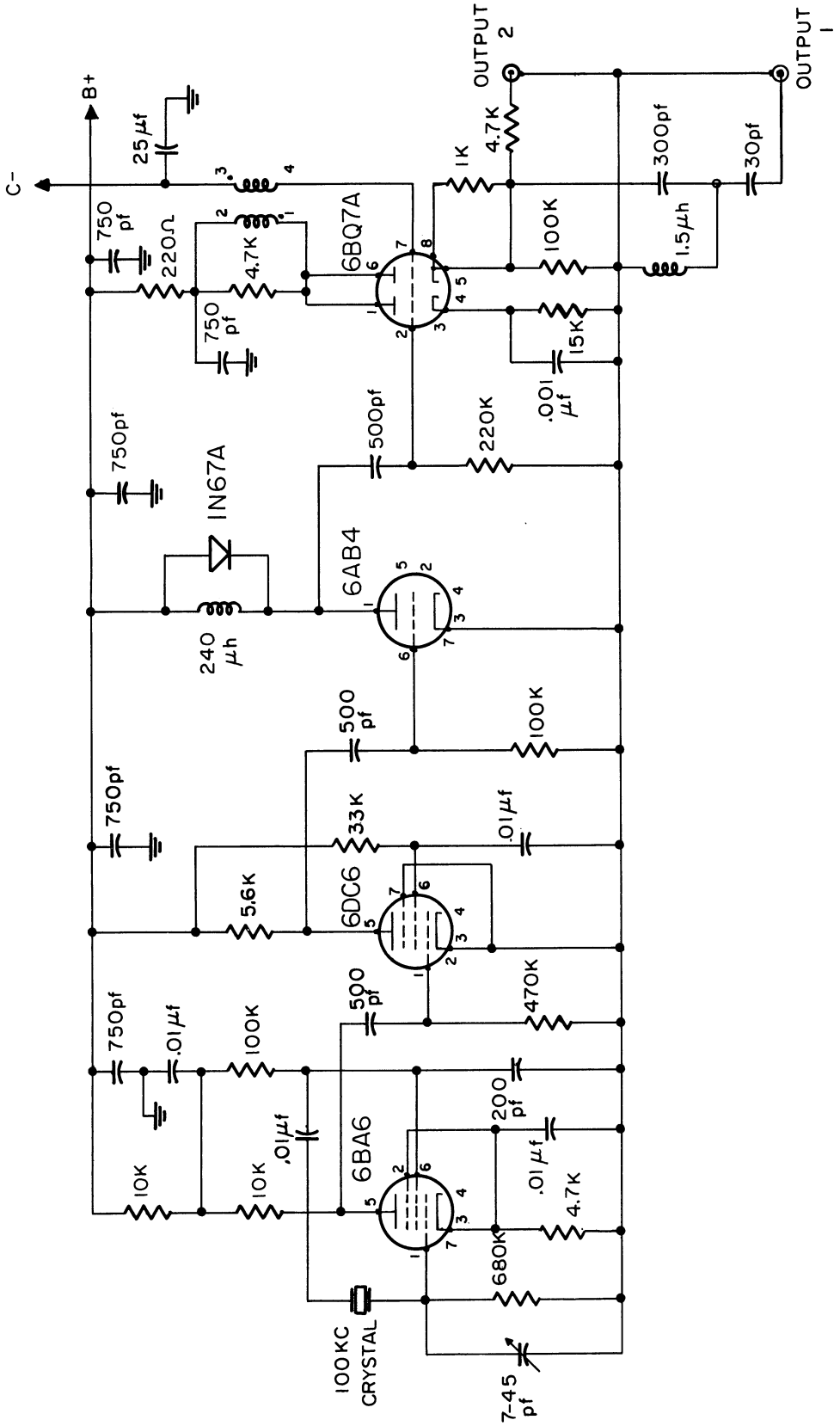

Fig. 27. Master crystal oscillator.

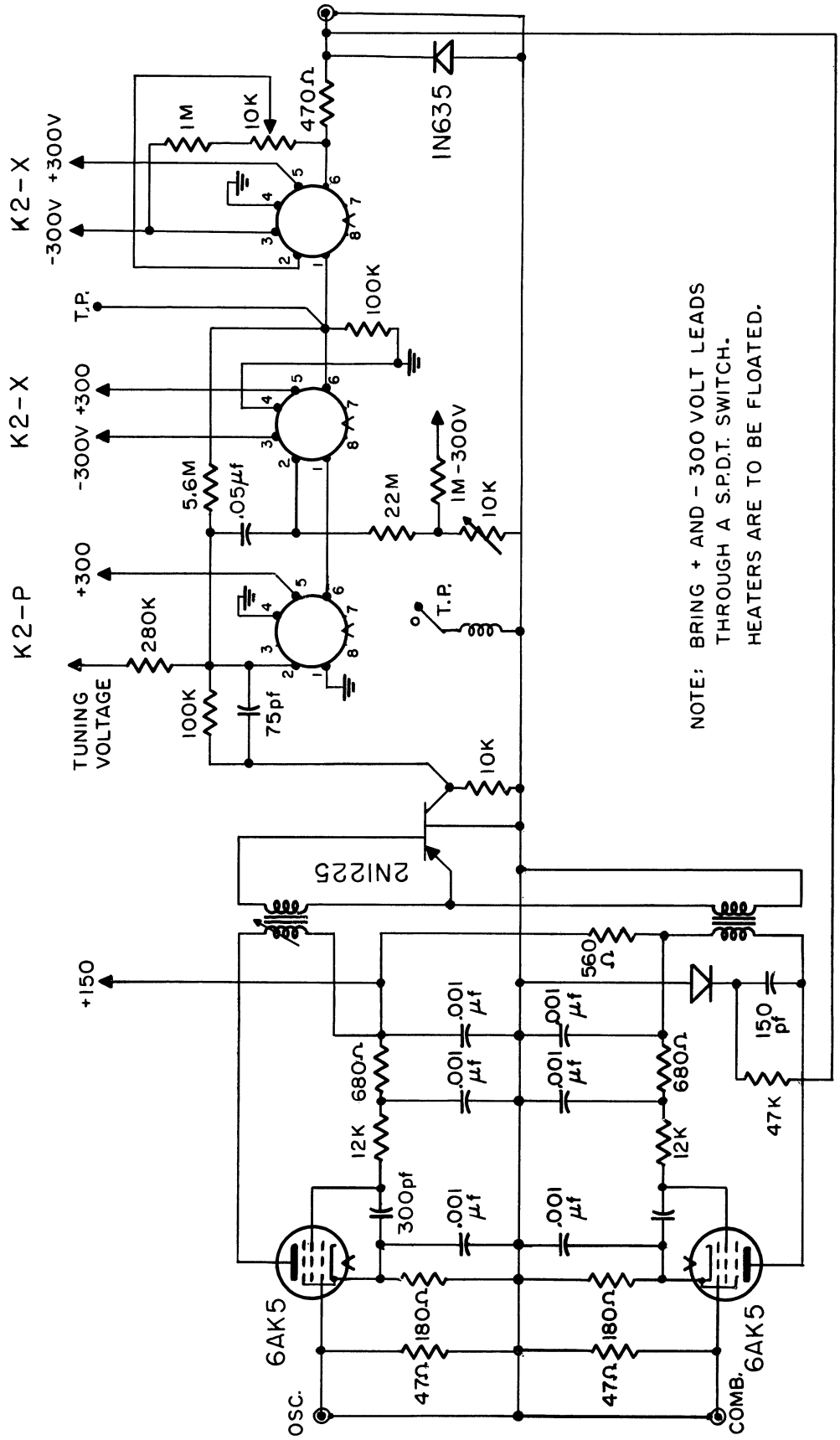

Fig. 28. Second discrete-frequency generator.

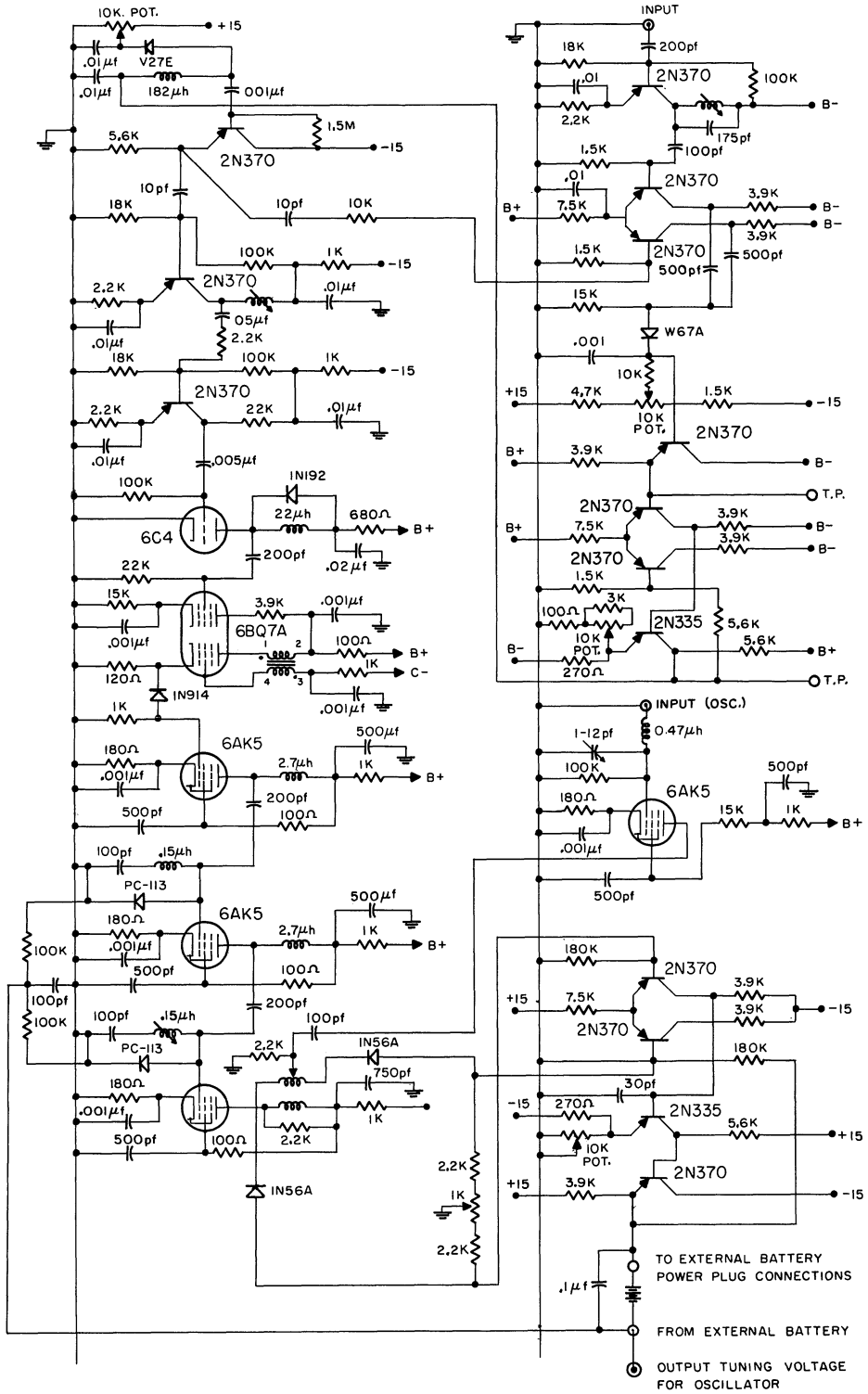

TO EXTERNAL BATTERY POWER PLUG CONNECTIONS

FROM EXTERNAL BATTERY

OUTPUT TUNING VOLTAGE FOR OSCILLATOR

Fig. 29. First discrete-frequency generator.

REFERENCES

1. T. W. Butler, Jr., "Generalized Frequency Synthesizer," Cooley Electronics Laboratory Technical Report No. 120, The University of Michigan, June 1961.

2. E. M. Aupperle, "A 1-Mc Transistor dc Amplifier," Cooley Electronics Laboratory Technical Memorandum No. 83, The University of Michigan, January 1961.

3. A. J. Viterbi, "Acquisition and Tracking Behavior of Phase-Lock Loops," External Publication No. 673, JPL, July 1959.

DISTRIBUTION LIST

Copy No.	
1-2	Commanding Officer, U. S. Army Signal Research and Development Laboratory, Fort Monmouth, New Jersey, ATTN: Senior Scientist, Electronic Warfare Division
3	Commanding General, U. S. Army Electronic Proving Ground, Fort Huachuca, Arizona, ATTN: Director, Electronic Warfare Dept.
4	Chief, Research and Development Division, Office of the Chief Signal Officer, Department of the Army, Washington 25, D. C., ATTN: SIGEB
5	Commanding Officer, Signal Corps Electronic Research Unit, 9560th USASRU, P. O. Box 205, Mountain View, California
6	U. S. Atomic Energy Commission, 1901 Constitution Avenue, N.W., Washington 25, D. C., ATTN: Chief Librarian
7	Director, Central Intelligence Agency, 2430 E Street, N.W., Washington 25, D. C., ATTN: OCD
8	Signal Corps Liaison Officer, Lincoln Laboratory, Box 73, Lexington 73, Massachusetts, ATTN: Col. Clinton W. Janes
9-18	Commander, Armed Services Technical Information Agency, Arlington Hall Station, Arlington 12, Virginia
19	Commander, Air Research and Development Command, Andrews Air Force Base, Washington 25, D. C., ATTN: SCRC, Hq.
20	Directorate of Research and Development, USAF, Washington 25, D. C., ATTN: Chief, Electronic Division
21-22	Hqs., Aeronautical System Division, Air Force Command, Wright Patterson Air Force Base, Ohio, ATTN: WWAD
23	Hqs., Aeronautical System Division, Air Force Command, Wright Patterson Air Force Base, Ohio, ATTN: WCLGL-7
24	Hqs., Aeronautical System Division, Air Force Command, Wright Patterson Air Force Base, Ohio - For retransmittal to - Packard Bell Electronics, P. O. Box 337, Newbury Park, California
25	Commander, Air Force Cambridge Research Center, L. G. Hanscom Field, Bedford, Massachusetts, ATTN: CROTLR-2
26-27	Commander, Rome Air Development Center, Griffiss Air Force Base, New York, ATTN: RCSSLD - for retransmittal to Ohio State University Research Foundation
28	Commander, Air Proving Ground Center, ATTN: Adj/Technical Report Branch, Eglin Air Force Base, Florida
29	Chief, Bureau of Naval Weapons, Code RRR-E, Department of the Navy, Washington 25, D. C.
30	Chief of Naval Operations, EW Systems Branch, OP-35, Department of the Navy, Washington 25, D. C.
31	Chief, Bureau of Ships, Code 691C, Department of the Navy, Washington 25, D. C.
32	Chief, Bureau of Ships, Code 684, Department of the Navy, Washington 25, D. C.
33	Chief, Bureau of Naval Weapons, Code RAAV-33, Department of the Navy, Washington 25, D. C.
34	Commander, Naval Ordnance Test Station, Inyokern, China Lake, California, ATTN: Test Director - Code 30
35	Director, Naval Research Laboratory, Countermeasures Branch, Code 5430, Washington 25, D. C.
36	Director, Naval Research Laboratory, Washington 25, D. C., ATTN: Code 2021
37	Director, Air University Library, Maxwell Air Force Base, Alabama, ATTN: CR-4987
38	Commanding Officer - Director, U. S. Naval Electronic Laboratory, San Diego 52, California
39	Office of the Chief of Ordnance, Department of the Army, Washington 25, D. C., ATTN: ORDTU
40	Chief, West Coast Office, U. S. Army Signal Research and Development Laboratory, Bldg. 6, 75 S. Grand Avenue, Pasadena 2, California
41	Commanding Officer, U. S. Naval Ordnance Laboratory, Silver Springs 19, Maryland
42-43	Chief, U. S. Army Security Agency, Arlington Hall Station, Arlington 12, Virginia, ATTN: IADEV
44	President, U. S. Army Defense Board, Headquarters, Fort Bliss, Texas
45	President, U. S. Army Airborne and Electronics Board, Fort Bragg, North Carolina
46	U. S. Army Antiaircraft Artillery and Guided Missile School, Fort Bliss, Texas

DISTRIBUTION LIST (Cont.)

Copy No.	
47	Commander, USAF Security Service, San Antonio, Texas, ATTN: CLR
48	Chief, Naval Research, Department of the Navy, Washington 25, D. C., ATTN: Code 931
49	Commanding Officer, U. S. Army Security Agency, Operations Center, Fort Huachuca, Arizona
50	President, U. S. Army Security Agency Board, Arlington Hall Station, Arlington 12, Virginia
51	Operations Research Office, John Hopkins University, 6935 Arlington Road, Bethesda 14, Maryland, ATTN: U. S. Army Liaison Officer
52	The John Hopkins University, Radiation Laboratory, 1315 St. Paul Street, Baltimore 2, Maryland, ATTN: Librarian
53	Stanford Electronics Laboratories, Stanford University, Stanford, California, ATTN: Applied Electronics Laboratory Document Library
54	HRB - Singer, Inc., Science Park, State College, Pennsylvania, ATTN: R. A. Evans, Manager, Technical Information Center
55	ITT Laboratories, 500 Washington Avenue, Nutley 10, New Jersey, ATTN: Mr. L. A. DeRosa, Div. R-15 Lab.
56	Director, USAF Project Rand, via Air Force Liaison Office, The Rand Corporation, 1700 Main Street, Santa Monica, Calif.
57	Stanford Electronics Laboratories, Stanford University, Stanford, California, ATTN: Dr. R. C. Cumming
58	Willow Run Laboratories, The University of Michigan, P. O. Box 2008, Ann Arbor, Michigan, ATTN: Dr. Boyd
59	Stanford Research Institute, Menlo Park, California, ATTN: Dr. Cohn
60-61	Commanding Officer, U. S. Army Signal Missile Support Agency, White Sands Missile Range, New Mexico, ATTN: SIGWS-EW and SIGWS-FC
62	Commanding Officer, U. S. Naval Air Development Center, Johnsville, Pennsylvania, ATTN: Naval Air Development Center Library
63	Commanding Officer, U. S. Army Signal Research and Development Laboratory, Fort Monmouth, New Jersey, ATTN: U. S. Marine Corps Liaison Office, Code AO-4C
64	President, U. S. Army Signal Board, Fort Monmouth, New Jersey
65-73	Commanding Officer, U. S. Army Signal Research and Development Laboratory, Fort Monmouth, New Jersey ATTN: 1 Copy - Director of Research 1 Copy - Technical Documents Center ADT/E 1 Copy - Chief, SIGRA/SL-SES 1 Copy - Chief, SIGRA/SL-SEA 1 Copy - Chief, SIGRA/SL-SEJ 1 Copy - File Unit No. 2, Mail and Records, Electronic Warfare Division 3 Cpys - Chief, Security Division (for retransmittal to BJSM)
74	Director, National Security Agency, Fort George G. Meade, Maryland, ATTN: TEC
75	Dr. B. F. Barton, Director, Cooley Electronics Laboratory, University of Michigan Research Institute, Ann Arbor, Michigan
76-99	Cooley Electronics Laboratory Project File, University of Michigan Research Institute, Ann Arbor, Michigan
100	Project File, The University of Michigan Office of Research Administration, Ann Arbor, Michigan

Above distribution is effected by Electronic Warfare Division, Surveillance Department, USASRDL, Evans Area, Belmar, New Jersey. For further information contact Mr. I. O. Myers, Senior Scientist, Telephone 59-61252.